COMPARISON OF BEAM DATA FOR DIFFERENT DETECTORS OF A 6 MV PHOTON BEAM

THEPPHITHAK WATTHANASARN

A THESIS SUBMITTED IN PARTIAL FULFILLMENT
OF THE REQUIREMENTS
FOR THE DEGREE OF MASTER OF SCIENCE
(MEDICAL PHYSICS)
FACULTY OF GRADUATE STUDIES
MAHIDOL UNIVERSITY
2008

Thesis

Entitled

COMPARISON OF BEAM DATA FOR DIFFERENT DETECTORS OF A 6 MV PHOTON BEAM

…………………………………
Mr. Thepphithak Watthanasarn
Candidate

…………………………………
Lect. Puangpen Tangboonduangjit,
Ph.D. (Medical Radiation Physics)
Major-Advisor

…………………………………
Assoc. Prof. Sivalee Suriyapee
M.Eng. (Nuclear Technology)
Co-Advisor

…………………………………
Asst. Prof. Chirapha Tannanonta,
M.Sc. (Medical Physics)
Co-Advisor

…………………………………..
Asst.Prof. Auemphorn Mutchimwong,
Ph.D.
Acting Dean
Faculty of Graduate Studies

………………………………..
Assoc. Prof. Vipa Boonkitticharoen,
Ph.D. (Radiation Biology)
Chair
Master of Science Programme
In Medical Physics
Faculty of Medicine
Ramathibodi Hospital

Thesis

Entitled

COMPARISON OF BEAM DATA FOR DIFFERENT DETECTORS OF A 6 MV PHOTON BEAM

was submitted to the Faculty of Graduate Studies, Mahidol University

for the degree of Master of Science (Medical Physics)

on

31 October, 2008

…………………………………
Mr. Thepphithak Watthanasarn
Candidate

…………………………………
Assoc. Prof. Vipa Boonkitticharoen,
Ph.D. (Radiation Biology)
Chair

…………………………………
Asst. Prof. Chirapha Tannanonta,
M.Sc. (Medical Physics)
Member

…………………………………
Lect. Puangpen Tangboonduangjit,
Ph.D. (Medical Radiation Physics)
Member

…………………………………
Assoc. Prof. Sivalee Suriyapee
M.Eng. (Nuclear Technology)
Member

…………………………………..
Asst. Prof. Auemphorn Mutchimwong,
Ph.D.
Acting Dean
Faculty of Graduate Studies
Mahidol University

………………………………..
Prof. Rajata Rajatanavin,
M.D., F.A.C.E.
Dean
Faculty of Medicine
Ramathibodi Hospital,
Mahidol University

ACKNOWLEDGEMENTS

The success of this thesis can been attributed to the extensive support and assistance from my major advisor, Dr. Puangpen Tangboonduangjit and my co-advisor, Asst. Prof. Chirapha Tannanonta. I deeply thank them for their valuable advice and guidance in this research.

I wish to thank Dr. Chaiyaporn kanka, director of Lopburi Cancer Center and Mr. Somsak Khaunchana, head of the Department of Radiotherapy, for kindness in examining the research instrument and providing suggestions for improvement.

I am grateful to all the lecturers and staff of the Radiotherapy Department of Lopburi cancer Center for their valuable advice and thanks also go to my friends in the Lopburi Cancer Center for their kind support.

Finally, I am grateful to my family for their financial support, entirely care, and love. The usefulness of this thesis, I dedicate to my wife and all the teachers who have taught me since my childhood.

Thepphithak Watthanasarn

COMPARISON OF BEAM DATA FOR DIFFERENT DETECTORS OF A 6 MV PHOTON BEAM

THEPPHITHAK WATTHANASARN 4637066 RAMP/M

M.Sc. (MEDICAL PHYSICS)

THESIS ADVISOR: PAUNGPEN TUNGBOONDAUNDJIT, Ph.D. (MEDICAL PHYSICS), JEERAPA TUNNANOON, M.Sc. (MEDICAL PHYSICS), SIVALEE SURIYAPEE, M.Eng. (NUCLEAR TECHNOLOGY)

ABSTRACT

The aim of this work was to investigate the different radiation detectors of Lopburi Cancer Center by comparing the beam data measurement: output factor, beam profile, and depth dose for field sizes between 2×2 cm^2 to 30×30 cm^2 at the depth of 1.5, 5, and 10 cm for 100 cm SSD in a 6 MV photon beam. For output factor measurements, IC 0.3 cm^3, Markus parallel plate chamber, and diode were used with respect to IC 0.6 cm^3 due to its air equivalence. However for beam profile and depth dose measurements, IC 0.3 cm^3, Markus parallel plate chamber were used with respect to the diode measurement due to its high spatial resolution as compared with XV film for some field sizes and depths. The IC 0.3 cm^3 and Markus parallel plate chamber are suitable for output measurement except for field sizes smaller than 3×3 cm^2. The IC 0.6 cm^3 underestimated the output factor for 2×2 cm^2 about 24.3% compared with IC 0.3 cm^3 due to it suffers from the volume averaging effect. For results concerning beam profile and surface dose measurement, both IC 0.3 cm^3 and Markus parallel plate chamber were not suitable due to their finite size of the sensitive volume. The maximum penumbra width difference was about 3 mm and the maximum surface dose for difference was about 3.7% and 9.4% for IC 0.3 cm^3 and Markus parallel plate chamber respectively at the field size of 2×2 cm^2 compared with diode measurement. Diode is highly suitable for a routine use of beam profile and depth dose measurement although diode is slightly over-response at the distal region of the depth dose curve and the penumbra tail due to its non tissue equivalence.

KEY WORDS : BEAM DATA MEASUREMENT/ DETECTORS/ DIODE/ RADIOTHERAPY

49 pp.

การเปรียบเทียบหัววัดรังสีในการวัดลำรังสีโฟตอนพลังงาน 6 MV

COMPARISON OF BEAM DATA FOR DIFFERENT DETECTORS OF A 6 MV PHOTON BEAM

เทพพิทักษ์ วัฒนสาร 4637066 RAMP/M

วท.ม. (ฟิสิกส์การแพทย์)

คณะกรรมการควบคุมวิทยานิพนธ์ : พวงเพ็ญ ตั้งบุญดวงจิต, Ph.D. (Medical Radiation Physics) , จีระภา ตันนานนท์, M.Sc. (Medical Physics) , ศิวลี สุริยาปี, M.Eng. (Nuclear Technology)

บทคัดย่อ

วัตถุประสงค์ในการวิจัยเพื่อศึกษาคุณสมบัติของหัววัดรังสีของศูนย์มะเร็งลพบุรีในการวัดคุณสมบัติของลำรังสีทั้งค่า output percentage depth dose และ beam profile ทำการวัดลำรังสีขนาดตั้งแต่ 2× 2 ตารางเซนติเมตร ถึง 30 × 30 ตารางเซนติเมตร ที่ความลึก 1.5 5 และ 10 เซนติเมตร โดยจัดระยะ source skin distance เท่ากับ 100 เซนติเมตร ใช้โฟตอนพลังงาน 6 MV

การวัดค่า Output ใช้หัววัดรังสีชนิด IC 0.3 cm^3 Plane parallel และ diode เทียบกับ IC 0.6 cm^3 ที่เป็นหัววัดรังสีอ้างอิง ส่วนการวัด beam profile และ percentage depth dose ใช้หัววัดรังสีชนิด IC 0.3 cm^3 และ plane parallel เทียบกับ diode เพราะ diode มีค่า high spatial resolution ซึ่งได้ทำการปรับเทียบกับ XV film ในบางขนาดของลำรังสีและบางความลึกแล้ว

จากผลการวิจัยพบว่าหัววัดรังสีชนิด IC 0.3 cm^3 และ Plane parallel เหมาะสมในการวัดค่า Output ที่ขนาดของลำรังสีน้อยกว่า 3× 3 ตารางเซนติเมตร ส่วนหัววัดรังสีชนิด IC 0.6 cm^3 จะเกิด underestimate เนื่องจากเกิด volume averaging effect ส่วนการวัดค่า beam profile และ percentage depth dose พบว่า IC 0.3 cm^3 และ Plane parallelไม่เหมาะสมในการวัดเพราะมีค่า penumbra มากกว่าของ diode ประมาณ 3 มิลลิเมตร ส่วนค่าปริมาณรังสีที่ผิวจะมีค่าความแตกต่างประมาณ 3.7% สำหรับหัววัดรังสีชนิด IC 0.3 cm^3 และประมาณ 9.4% สำหรับหัววัดรังสีชนิด Plane parallelที่ขนาดลำรังสี 2× 2 ตารางเซนติเมตร ส่วนหัววัดรังสีชนิด diode จะเหมาะสมในการวัดปริมาณรังสีในการวัด beam profile และ percentage depth dose ที่ขนาดลำรังสีเล็ก ส่วนขนาดลำรังสีที่เพิ่มขึ้นและที่ความลึกมากขึ้น หัววัดรังสีชนิด diode จะไม่เหมาะสมในการวัดเพราะเกิดการตอบสนองค่าการวัดที่เกินความเป็นจริงจากคุณสมบัติของหัววัดรังสีเองคือมีค่าความหนาแน่นไม่เทียบเท่าค่าความหนาแน่นของเนื้อเยื่อ

49 หน้า

CONTENTS

LIST OF TABLES

LIST OF FIGURES

LIST OF ABBREVIATIONS

Abbreviations	Term
3D-conformal	three dimensions conformal
RTPS	The Radiation Treatment Planning System
PDD	Percentage Depth Dose
SSD	Source Skin Distance
SAD	Source Axis Distance
OAR	The Off-axis Ratio
OD	Optical Density
IC	Ionization Chamber
DVH	Dose Volume Histogram
OF	Output Factor
PTV	Plan Target Volume
TMR	The tissue maximum ratio

CHAPTER I

INTRODUCTION

The aim of the radiotherapy for cancer treatment is to delivers the maximum dose into the cancer cell[1] while keeping the normal cell to the minimum dose. Therefore the trend for changing conventional techniques to 3D-conformal treatment techniques has emerged into many institutions including Lopburi Cancer Center.

Lopburi Cancer Center has treated cancer patients with the radiotherapy since 1995. Their instruments include cobalt-60, cesium-137 for brachytherapy and linear accelerator 6 MV. The majority of cancer patients have been treated successfully using 2D-conformal technique however the requirement for higher technology machines to achieve more conformal dose distribution is still demanded. Therefore, in the near future, the Cancer Center will obtain the new machine which provides the capability to treat cancer patients using 3D-conformal technique.

Nevertheless in order to accomplish 3D conformal radiotherapy, it does not rely on the modern machine but also the accurate beam data required for radiation treatment planning system (RTPS) to generate accurately the isodose distribution.

The measurement of the beam data depends on the requirements of the manufacturer of the RTPS. However in order to obtain the correct beam data, the detectors performing the measurement is critically important.

Beam data[2] is the collection of the dosimetric measurement which is the input for RTPS to create isodose distribution. The main collections of beam data are the percentage depth dose, output factor, and beam profile.

Percentage depth dose (PDD)[3]

Central axis dose distributions inside the patient or phantom are usually normalized to D_{max} = 100% at the depth of dose maximum z_{max} and then referred to as the PDD distributions. The depths of dose maximum and the surface dose of the PDD depend on the beam energy (hν); the larger the beam energy, the larger the depths of dose maximum and the lower the surface dose. For constant depth (z), SSD (f) and energy (hν), the PDD increases with increasing field size (A) because of increased scatter contribution to points on the central axis. An example for a ^{60}Co beam is given in Table 1.1. For constant z, A and hν the PDD increases with increasing f because of a decreasing effect of z on the inverse square factor, which governs the primary component of the photon beam. An example for a ^{60}Co beam is given in Table 1.2. For constant z, A and f, the PDD beyond z_{max} increases with beam energy because of a decrease in beam attenuation (i.e. because of an increase in beam penetrating power). An example of PDDs distributions for 10 × 10 cm^2 fields and various megavoltage photon beams is given in Figure 1.1 and Table 1.3. The size of the buildup region increases with beam energy and the surface dose decreases with beam energy. PDDs for radiotherapy beams are usually tabulated for square fields; however, the majority of fields used in radiotherapy are rectangular or irregularly shaped. The concept of equivalent squares is used to determine the square field that will be equivalent to the given rectangular or irregular field.

Table 1.1 Percentage depth doses for a cobalt-60 beam in water for various field sizes and an SSD of 100 cm. (Podgorsak EB. External photon beam: Physical aspects. In: Podgorsak EB. Radiation oncology physics: a handbook for teachers and students. Vienna: IAEA; 2005.p.182.)

	A (cm^2)						
	0 × 0	5 × 5	10 × 10	15 × 15	20 × 20	25 × 25	50 × 50
PDD(5, A, 100, Co)	68.2[a]	76.7	80.4	82.0	83.0	83.4	85.2
PDD(10, A, 100, Co)	44.7[a]	53.3	58.7	61.6	63.3	64.4	67.3
PDD(15, A, 100, Co)	29.5[a]	36.5	41.6	44.9	47.1	48.6	49.7

[a] Calculated using Eq. (6.35) with μ_{eff} = 0.0657 cm^{-1}.

Table 1.2 Percentage depth doses for a cobalt-60 beam in water for various source to surface distances, depth Z of 5 cm in a phantom and a field of A=10×10 cm^2. (Podgorsak EB. External photon beam: Physical aspects. In: Podgorsak EB. Radiation oncology physics: a handbook for teachers and students. Vienna: IAEA; 2005.p.182.)

f = SSD (cm)	60	80	100	120	140
PDD(5, 10, f, Co)	76.2	78.8	80.0	81.3	82.3

Table 1.3 Percentage depth doses for various photon beams in a water phantom with a field size A of 10×10 cm^2, an SSD of 100 cm and two depths: 5 cm and 10 cm.

(Podgorsak EB. External photon beam: Physical aspects. In: Podgorsak EB. Radiation oncology physics: a handbook for teachers and students. Vienna: IAEA; 2005.p.183.)

	Photon beam $h\nu$					
	Co-60	4 MV	6 MV	10 MV	18 MV	25 MV
Nominal z_{max} (cm)	0.5	1.0	1.5	2.5	3.5	5.0
PDD(5, 10, 100, $h\nu$)	80	84	86	92	97	98
PDD(10, 10, 100, $h\nu$)	59	65	67	74	80	82

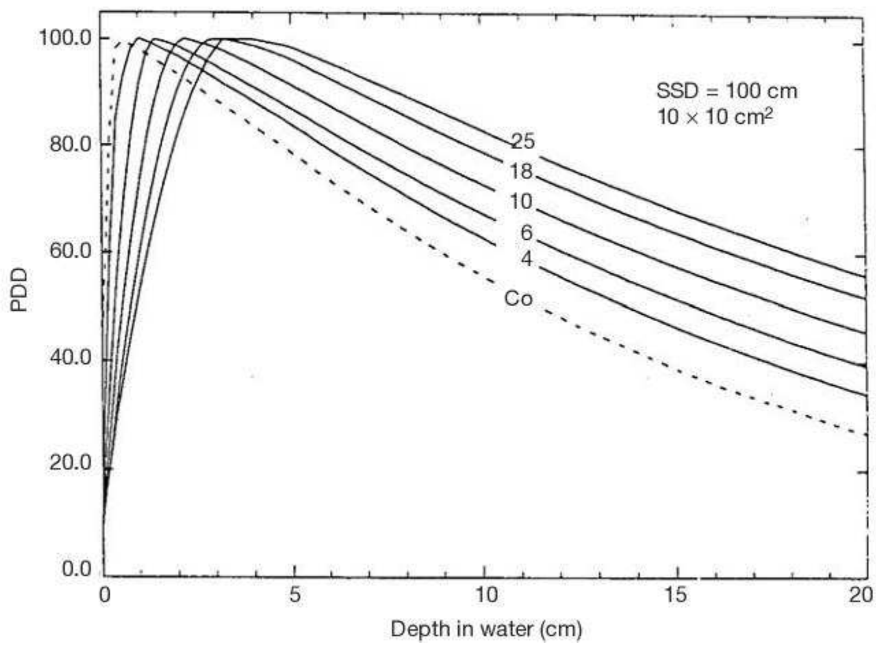

Figure 1.1 PDD curves in water for a 10 × 10 cm^2 field at an SSD of 100 cm for various megavoltage photon beams ranging from ^{60}Co γ ray to 25 MV X-rays.

(Podgorsak EB. External photon beam: Physical aspects. In: Podgorsak EB. Radiation oncology physics: a handbook for teachers and students. Vienna: IAEA; 2005.p.182.)

Output factor[3]

For a given photon beam at a given SSD, the dose rate at point P (at depth z_{max} in a phantom) depends on the field size A; the larger the field size, the larger the dose. Out put in air is most commonly called collimator scatter factor or headscatter factor. Exposure in air, air kerma in air and 'dose to small mass of medium in air' at a given point P in air contain contributions from two components: primary and scatter. The primary component is the major component; it comes directly from the source and does not depend on the field size. Scatter represents a minor yet non-negligible component; it consists of photons scattered into point P mainly from the collimator but also possibly from the air and the flattening filter of a linac. The scatter component depends on field size A (collimator setting): the larger the field size, the larger the collimator surface available for scattering and consequently the larger the scatter component.

Beam profile[3]

The beam profiles measured perpendicularly to the beam central axis at a given depth in a phantom. The depths of measurement are typically at z_{max} and 10 cm for verification of compliance with machine specifications, in addition to other depths required by the particular radiation treatment planning system (RTPS) used in the department. An example of typical dose profiles measured at various depths in water for two field sizes (10 × 10 and 30 × 30 cm^2) and a 10 MV X ray beam is shown in Figure 1.2. Combining a central axis dose distribution with off-axis data results in a volume dose matrix that provides 2-D and 3-D information on the dose distribution. The off-axis ratio (OAR) is usually defined as the ratio of dose at an off-axis point to the dose on the central beam axis at the same depth in a phantom.

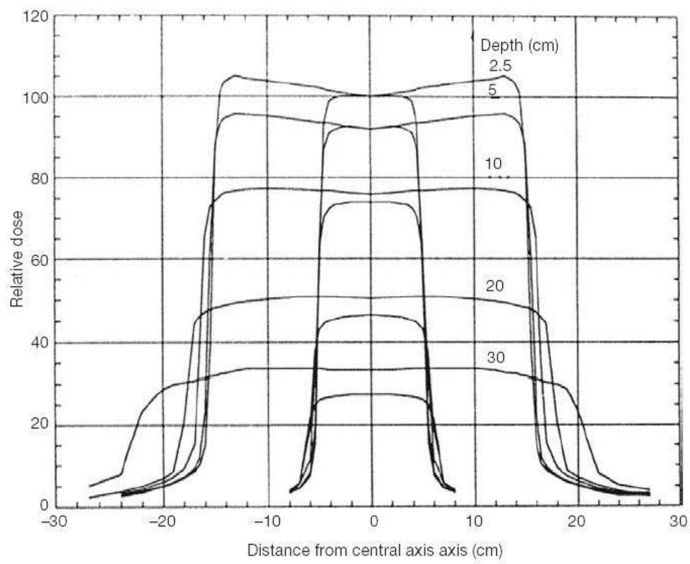

Figure 1.2 An example of beam profiles for two field sizes (10 × 10 cm^2 and 30 × 30 cm^2) and a 10 MV X-ray beam at various depths in water. The central axis dose values are scaled by the appropriate PDD value for the two fields. (Podgorsak EB. External

photon beam: Physical aspects. In: Podgorsak EB. Radiation oncology physics: a handbook for teachers and students. Vienna: IAEA; 2005.p.195.)

Megavoltage X ray beam profiles consist of three distinct regions: central, penumbra and umbra. The central region represents the central portion of the profile extending from the beam central axis to within 1-1.5 cm from the geometric field edges of the beam. The geometric field size, indicated by the optical light field, is usually defined as the separation between the 50% dose level points on the beam profile. In the central region, the beam profile for ^{60}Co beams is affected by the inverse square dose fall-off as well as by increased phantom thickness for off-axis points. For linacs, on the other hand, the central region of the beam profile is affected by the energy of electrons striking the thick target, by the target atomic number and by the flattening filter atomic number and geometric shape. In the penumbral region of the dose profile the dose changes rapidly and depends also on the field defining collimators, the finite size of the focal spot (source size) and the lateral electronic disequilibrium. The dose fall-off around the geometric beam edge is sigmoid in shape and extends under the collimator jaws into the penumbral tail region, where there is a small component of dose due to the transmission through the collimator jaws (transmission penumbra), a component attributed to finite source size (geometric penumbra) and a significant component due to in-patient X-ray scatter (scatter penumbra). The total penumbra is referred to as the physical penumbra and is the sum of the three individual penumbras: transmission, geometric and scatter. The physical penumbra depends on beam energy, source size, SSD, source to collimator distance and depth in a phantom. Umbra is the region outside the radiation field, far removed from the field edges. The dose in this region is generally low and results from radiation transmitted through the collimator and head shielding.

Dose profile uniformity is usually measured by a scan along the center of both major beam axes for various depths in a water phantom. Two parameters that quantity field uniformity is then determined: field (beam) flatness and field (beam) symmetry.

The beam flatness (F) is assessed by finding the maximum D_{max} and minimum D_{min} dose point values on the beam profile within the central 80% of the beam width and then using the relationship:

$$F = 100 \times \frac{D_{\max} - D_{\min}}{D_{\max} + D_{\min}} \qquad \textbf{(1)}$$

Standard linear accelerator specifications generally require that F be less than 3% when measured in a water phantom at a depth of 10 cm and an SSD of 100 cm for the largest field size available (usually 40 × 40 cm^2).

Compliance with the flatness specifications at a depth of 10 cm in water results in 'over-flattening' at z_{max}, which manifests itself in the form of 'horns' in the profile, and in 'under-flattening', which progressively worsens as the depth z increases from 10 cm to larger depths beyond 10 cm, as evident from the profiles for the 30 × 30 cm^2 field in Fig. 2. The typical limitation on beam horns in the z_{max} profile is 5% for a 40 × 40 cm^2 field at SSD= 100 cm. The over-flattening and under-flattening of the beam profiles is caused by the lower beam effective energies in off-axis directions compared with those in the central axis direction.

The beam symmetry (S) is usually determined at z_{max}, which represents the most sensitive depth for assessment of this beam uniformity parameter. A typical symmetry specification is that any two dose points on a beam profile, equidistant from the central axis point, are within 2% of each other. Alternatively, areas under the z_{max} beam profile on each side (left and right) of the central axis extending to the 50% dose level (normalized to 100% at the central axis point) are determined and S is then calculated from:

$$S = 100 \times \frac{\text{area}_{\text{left}} - \text{area}_{\text{right}}}{\text{area}_{\text{left}} + \text{area}_{\text{right}}} \qquad \textbf{(2)}$$

The areas under the z_{max} profiles can often be determined using an automatic option on the water tank scanning device (3-D isodose plotter). Alternatively, using a planimeter or even counting squares on graph paper with a hard copy of the profile are practical options.

The good characteristics of the radiation detector are as following[4].

1. Accuracy and precision. The accuracy of dosimetry measurements is the proximity of their expectation value to the ‘true value’ of the measured quantity. The precision of dosimetry measurements specifies the reproducibility of the measurements under similar conditions and can be estimated from the data obtained in repeated measurements. High precision is associated with a small standard deviation of the distribution of the measurement results.
2. Linearity. Ideally, the dosimeter reading M should be linearly proportional to the dosimetric quantity Q. If it is not the case then the correction factor need to be applied.
3. Dose rate dependence. Integrating systems measure the integrated response of a dosimetry system. For such systems the measured dosimetric quantity should be independent of the rate of that quantity. However the correction factor needs to be employed if the detector depends on the dose rate.
4. Directional dependence. Dosimeter usually exhibits directional dependence, due to its constructional details, physical size and the energy of the incident radiation. The directional correction factor needs to be used, especially the semiconductor dosimetry system for using in vivo measurement.

Ionization chamber dosimetry system[4]

An ionization chamber is basically a gas filled cavity surrounded by a conductive outer wall and having a central collecting electrode. The wall and the collecting electrode are separated with a high quality insulator to reduce the leakage current when a polarizing voltage is applied to the chamber.

A guard electrode is usually provided in the chamber to further reduce chamber leakage. The guard electrode intercepts the leakage current and allows it to flow to ground, bypassing the collecting electrode. It also ensures improved field uniformity in the active or sensitive volume of the chamber, with resulting advantages in charge collection.

Measurements with open air ionization chambers require temperature and pressure correction to account for the change in the mass of air in the chamber volume, which changes with the ambient temperature and pressure.

In this study, two types of ionization chamber dosimetry system were used.

Cylindrical (thimble/Farmer type) ionization chamber

Cylindrical chambers as shown in Figure 1.3 are produced by various manufacturers, with active volumes between 0.1 and 1 cm^3. They typically have an internal length no greater than 25 mm and an internal diameter no greater than 7 mm. The wall material is of low atomic number *Z* (i.e. tissue or air equivalent), with the thickness less than 0.1 g/cm^2. A chamber is equipped with a buildup cap with a thickness of about 0.5 g/cm^2 for calibration free in air using ^{60}Co radiation. The chamber construction should be as homogeneous as possible, although an aluminium central electrode of about 1 mm in diameter is typically used to ensure flat energy dependence.

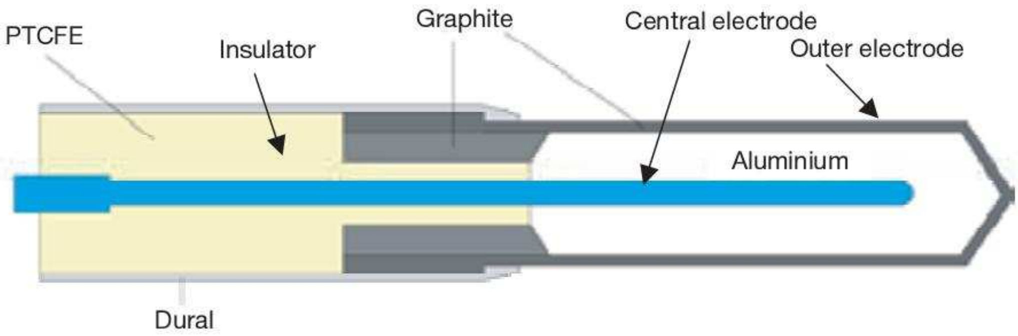

Figure 1.3 Basic design of a cylindrical Farmer type ionization chamber. (Izewska J, Rajan G. Radiation Dosimeters. In: Podgorsak EB. Radiation oncology physics: a handbook for teachers and students. Vienna: IAEA; 2005. p. 77.)

Parallel-plate (plane-parallel) ionization chambers

A parallel-plate ionization chamber consists of two plane walls, one serving as an entry window and polarizing electrode and the other as the back wall and collecting electrode, as well as a guard ring system. The back wall is usually a block of conducting plastic or a non-conducting material (usually Perspex or polystyrene) with a thin conducting layer of graphite forming the collecting electrode and the guard ring system on top. A schematic diagram of a parallel-plate ionization chamber is shown in Figure 1.4. The parallel-plate chamber is recommended for dosimetry of electron beams with energies below 10 MeV. It is also used for surface dose and depth dose measurements in the buildup region of megavoltage photon beams.

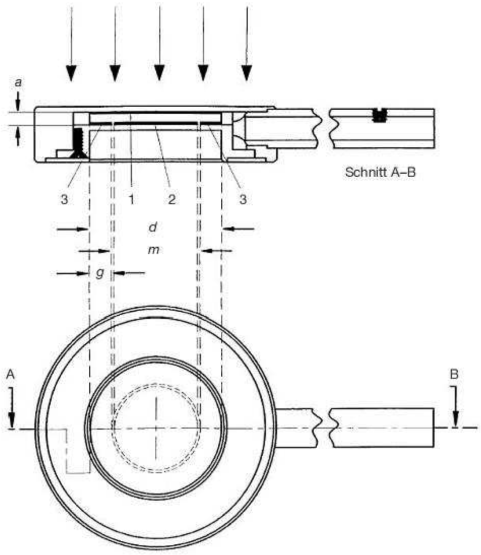

Figure 1.4 Parallel-plate ionization chamber. 1: the polarizing electrode. 2: the measuring electrode. 3: the guard ring. a: the height of the air cavity. d: the diameter of the polarizing electrode. m: the diameter of the collecting electrode. g: the width of the guard ring. (Izewska J, Rajan G. Radiation Dosimeters. In: Podgorsak EB. Radiation oncology physics: a handbook for teachers and students. Vienna: IAEA; 2005.p.80.)

Surface doses and doses in the buildup region for photon beams are measured with parallel-plate ionization chambers incorporating a thin polarizing electrode window (to be able to measure the surface dose) and a small electrode separation (typically 1 mm, for better spatial resolution). It was found that, in the buildup region the positive chamber polarity produces a larger signal than the negative polarity as shown in Figure 1.5. [3] The difference in signals is most pronounced on the phantom surface and then diminishes with depth until it disappears at depths of z_{max} and beyond.

At z_{max} and beyond this curve is more conveniently measured with small volume cylindrical ionization chamber; the results will match those obtained with a parallel-plate chamber. In the buildup region, however, the cylindrical chamber will read an unrealistically high signal because of its excessive wall thickness.

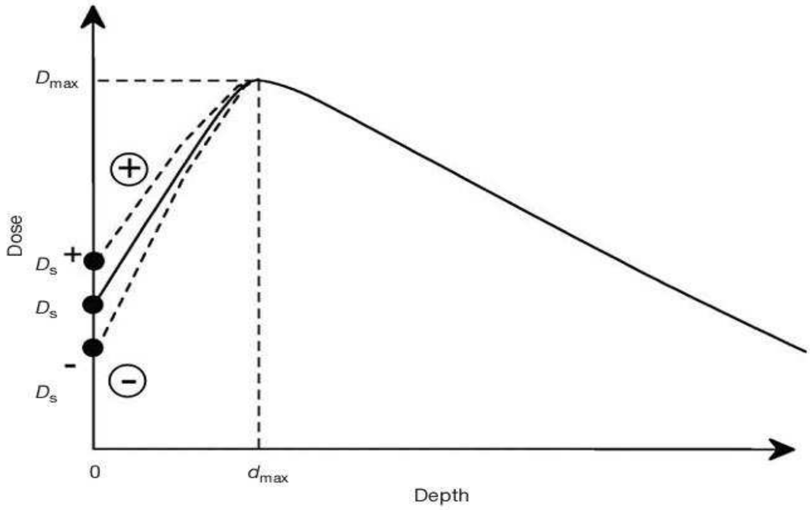

Figure 1.5 Megavoltage photon beam depth doses measured with a parallel-plate ionization chamber. In the buildup region the positive polarity produces a higher reading than the negative polarity; beyond z_{max} both polarities give essentially identical signals. (Podgorsak EB. External photon beam : Physical aspects. In: Podgorsak EB. Radiation oncology physics: a handbook for teachers and students. Vienna: IAEA; 2005. 210.)

Radiographic film

Radiographic X-ray film performs several important functions in diagnostic radiology, radiotherapy and radiation protection. It can serve as a radiation detector, a relative dosimeter, a display device and an archival medium. Unexposed X ray film consists of a base of thin plastic with a radiation sensitive emulsion (silver bromide (AgBr) grains suspended in gelatin) coated uniformly on one or both sides of the base. Ionization of AgBr grains, as a result of radiation interaction, forms a latent image in the film. This image only becomes visible (film blackening) and permanent subsequently to processing. Light transmission is a function of the film opacity and can be measured in terms of optical density (OD) with devices called densitometers. The OD is defined as OD = log10 (I_0/I) and is a function of dose. I_0 is the initial light intensity and I is the intensity transmitted through the film. Film gives excellent 2-D spatial resolution and, in a single exposure, provides information about the spatial distribution of radiation in the area of interest or the attenuation of radiation by intervening objects. The useful dose range of film is limited and the energy dependence is pronounced for lower energy photons. The response of the film depends on several parameters, which are difficult to control. Consistent processing of the film is a particular challenge in this regard. Typically, film is used for qualitative dosimetry, but with proper calibration, careful use and analysis film can also be used for dose evaluation.

Silicon diode dosimetry systems

A silicon diode dosimeter is a p–n junction diode. The diodes are produced by taking n type or p type silicon and counter-doping the surface to produce the opposite type material. These diodes are referred to as n–Si or p– Si dosimeters, depending upon the base material. Both types of diode are commercially available, but only the p–Si type is suitable for radiotherapy dosimetry, since it is less affected by radiation damage and has a much smaller dark current. Radiation produces electron–hole (e–h) pairs in the body of the dosimeter, including the depletion layer. The charges (minority charge carriers) produced in the body of the dosimeter, within the diffusion length, diffuse into the depleted region. They are swept across the depletion region under the action of the electric field due to the intrinsic potential. In this way a current is generated in the reverse direction in the diode. Diodes are used in the short circuit mode, since this mode exhibits a linear relationship between the measured charge and dose. They are usually operated without an external bias to reduce leakage current. Diodes are more sensitive and smaller in size than typical ionization chambers. They are relative dosimeters and should not be used for beam calibration, since their sensitivity changes with repeated use due to radiation damage. Diodes are particularly useful for measurement in phantoms, for example of small fields used in stereotactic radiosurgery or high dose gradient areas such as the penumbra region. They are also often used for measurements of depth doses in electron beams. For use with beam scanning devices in water phantoms, they are packaged in a waterproof encapsulation. When used in electron beam depth dose measurements, diodes measure directly the dose distribution (in contrast to the ionization measured by ionization chambers). Diodes show a variation in dose response with temperature (this is particularly important for long radiotherapy treatments), dependence of signal on the dose rate (care should be taken for different source to skin distances), angular (directional) dependence and energy dependence even for small variations in the spectral composition of radiation beams (important for the measurement of entrance and exit doses).

CHAPTER II
OBJECTIVES

Research question

Whether or not the detectors of Lopburi Cancer Center are suitable for beam data measurement?

The objectives of the study are as followed:

To investigate the different detectors in measurement of the photon beam of Lopburi Cancer Center by comparing the beam data measurements.

CHAPTER III
LITERATURE REVIEW

Garcia-Vicente C et al[5] determined the effect of the detector size when planning three-dimensional conformal radiation therapy (3D-CRT) treatments. They found that organs at risk (OAR) received higher dose levels when a 5.5 mm detector (0.6 cc ionization chamber) was used to measure profiles compared to the case in which a 2.0 mm detector (PFD^{3G} diode) was used. That was because of the errors in the measured penumbra of beam profiles by the large detector size. Therefore to avoid this overirradiation to the organs at risk, the measured profiles should be acquired with a suitable detector size (2-3 mm active diameter). In this study, the appropriate detector is PFD^{3G} diode with a 2.0 mm diameter detector for the case of 3D-CRT.

F Haryanto et al[6] investigated beam output factors (OF), beam profile and depth dose curve using various detectors (diode, diamond, pinpoint, and ionization chamber). Their sizes are shown in Table 3.1.

Table 3.1: The dimensions of various detectors. (Haryanto F,Fippel M, Laub W, Dohm O, Nusslin F. Investigation of Photon beam output factors for conformal radiation therapy-Monte Carlo simulations and measurements. Phys Med Biol 2002; 47 : N133-N143.)

Detectors	Manufacturer	Thickness	Surface area	Volume
Diamond		0.25 mm	5.6 mm^2	
Diode	PTW-Freiburg, type 60008	2.5 µm	1 mm^2	
Pinpoint	PTW-Freiburg, type 31006	2mm in diameter and 5 mm in length		
Ionization chamber (IC)	PTW-Freiburg, type 31002			0.125 cm^3

The measurement was performed using linear accelerator photon energies 6 MV. The depth of measurement was 10 cm and SSD was 100 cm for field size ranging from 1 cm to 15 cm. There was an agreement within 3% for all detectors of OF measurement for field size larger than 2 cm. The largest difference was observed for 1×1 cm^2 between the OF measured with diode and ionization chamber which was found to be approximately 35% due to the detector size and the water equivalence of the detector material. In addition, ionization chamber results showed lower dose than pinpoint chamber results because volume of the ionization chamber is larger than that of pinpoint which leads to increasing lateral electronic disequilibrium. However pinpoint gave higher dose results for the largest fields due to the over-response of this detector to low energy scatter. Moreover OF measurement using diode is larger than that using diamond because diamond detector is better water equivalent than diode detector. In conclusion, the effect of various detectors to OF measurement for field size at least 2×2 cm can be negligible but not for field size 1×1 cm. The diamond detector seems to be the detector of choice for OF measurement for fields smaller than 2×2 cm because of small sensitive volume and its water equivalent. The depth dose measurement result agreed between diode and ionization measurement at 10×10 cm field size. Also the good agreement is the same as the beam profile comparison except the penumbra region. The ionization chamber penumbra measurement was larger than that of others due to the larger size of the sensitive volume of the ionization chamber.

M Bucciolini et al[7] investigated the agreement between PTW diamond detector with ionization chamber (Scanditronix RK chamber) and diode (Scanditronix p-type silicon diode) for output factor, percentage depth dose, and beam profile measurement. The dimensions of the detectors used are summarized in Table 3.2.

Table 3.2: Geometrical features of the employed dosimeters (Bucciolini M, Buonamici FB, Mazzocchi S, Angelis CD, Oniri S, Cirrone GAP. Diamond detector versus silicon diode and ion chamber in photon beams of different energy and field size. Med Phys 2003; 30: 2149-54.)

Diamond	PTW type 60003	Volume: 1.4×10^{-3} cc	Sensitive area: 4.5 mm^2	Sensitive volume thickness: 310 μm
Ionization chamber	Scanditronix RK	Volume: 0.12 cc	Cavity length: 10 mm	Cavity diameter: 4 mm
Si-diode	Scanditronix	Volume: 0.3×10^{-3} cc	Detector diameter: 2.5 mm	Sensitive volume thickness: 60 μm

They found that for output factor measurement, RK chamber showed underestimation of dose for small field size (2.6 cm) especially at higher energy (25 MV) due to the averaging effect of the ionization chamber. For percentage depth dose measurement, diode obtained over response for all field size at large depth (>14 cm) because the amount of scattered low energy photons increases with depth and the number of photoelectric interactions in silicon increases too. However it was not found for 25 MV due to a lower contribution of the photoelectric interaction. The ion chamber still overestimated dose in the smaller field size however it was less pronounce for large depth because of increasing the field dimensions. As expected, the RK ion chamber measured penumbras were slightly higher than those derived by the solid-state detectors. The diamond detector showed no averaging effect compared with ion chamber and no energy dependence effect compared with silicon diode detector. However there are some weak points for diamond detector such as dose rate dependence, need pre-irradiation dose for signal stability, and high cost but it is appropriate for smaller field size (<2.6 cm) in intensity modulated radiation therapy or stereotactic treatments.

Laub W. and Wong T.[8] investigated the effect of detector size (volume effect) in the dosimetry of small fields and of steep dose gradient regions in IMRT. The profile comparison for IMRT beams was found that a standard ionization chamber (IC) of 0.125 cm^3 gave broader penumbra due to the volume effect than film (0.2 mm). This can cause more than 10% to the local difference in dose values in the comparison between the treatment planning calculation and film measurement when using IC 0.125 cm^3 for the commissioning of treatment planning system. Moreover the deviations of measurements using the pinpoint chamber were much smaller than deviations of measurements using the Farmer chamber for the absolute point dose comparison. For the output factor measurement for small field sizes, IC obtained underestimation of the output factor measurement mostly due to lateral electron disequilibrium. However diode overestimate the output factor measurement because it is non-water equivalent leading to the increase of the secondary electrons. Therefore diamond detector was found to be suitable for output factor measurements of small fields because of its high spatial resolution and water equivalence.

Rustgi S.[9] evaluated the dosimetric properties of a diamond detector and compare them to that of a silicon p-type photon diode and a small volume ionization chamber. The dimensions of the detectors are shown in Table 3.3.

Table 3.3: The dimensions of the detectors. (Rustgi SN. Evaluation of the dosimetric characteristics of a diamond detector for photon beam measurements. Med Phys 1995; 22(5): 567-70.)

Detectors	Manufacturer	Volume	Sensitive area	Thickness
Diamond	PTW	1.9 mm^3	7.3 mm^2	0.26 mm
Diode	Scanditronics	0.3 mm^3	4.9 mm^2	0.06 mm
IC 10	Wellhofer	0.14 cm^3	Diameter 6 mm, length 3.3 mm	
Markus		Plate separation 22 mm, active diameter 5.4 mm		

He mentioned that the directional dependence of the radiation response of the diamond detector for cobalt 60, 6 MV and 18 MV photon beams was more uniform than that of the diode. However the spatial resolution of the diamond detector, as measured by penumbra width, was slightly larger than that of the diode detector but clearly smaller than to that of the 0.14 cm^3 ionization chamber. Also the tissue maximum ratio (TMR) measurements for small size photon fields (diameter $\leq$ 4 cm) with the diamond, diode, and a Markus parallel plate chamber were in excellent agreement.

As a result, selecting the appropriate detectors for measuring beam data correctly is the strong motivation for doing this research.

CHAPTER IV
MATERIALS AND METHODS

A. Materials

1. Linear accelerator

Varian type Clinac 2100 C/D linear accelerator offers five electron beam energies and two x-ray energies. The x-ray energies are 6 MV and 10 MV see figure 4.1. The electron energies range from 6 MeV to 20 MeV. X-ray field sizes range from 0.5×0.5 cm^2 to 40×40 cm^2, at a 100 cm target-to-skin distance, and electron field sizes from 4×4 cm^2 to 25×25 cm^2. Only photon beam energy of 6 MV was used in this research.

Figure 4.1 Varian 2100 C/D 6 and 10 MV for photon beam and 6, 9, 12, 16 and 20 MeV Electron beam

2. Detectors

The dosimetry diode type 6008 (PTW-Freiburg) is a p-type Si diode. Because of the high signal-to-noise ratio of the diode, see figure 4.2 (a), the effective measuring volume of the detector can be made small and allows data acquisition with a very good spatial resolution. The excellent spatial resolution makes it possible to measure very precisely beam profiles even in the penumbra region of small fields. The waterproof detector can be used in air, solid state phantom and in water. The detector features a small sensitive volume is 0.0025 mm^3 and a thickness of only 2.5 µm. The detector has reference point at on detector axis of 2 mm from detector trip. Another detector that is specifically designed for small sized for high spatial resolution is the plane parallel ionization chamber for the advanced markus chamber type 34045 (PTW Freiburg) as shown in Figure 4.2 (b). The sensitive volume of this ionization chamber is 0.02 cm^3. The detector is the successor of the well-known classic Markus electron chamber, equipped with a wide guard ring for perturbation-free measurements. The thin entrance window allows measurement in solid phantoms up to the surface. The protection cap makes the chamber waterproof for measurement in water phantoms.

The other detectors used in this study are the cylindrical ionization chambers. The first one is the 0.3 cm^3 semiflex chamber tube type 31013 (PTW-Freiburg), see figure 4.2 (c), with a uniform spatial resolution during phantom measurements along all three axes and designed for relative dose measurement. The second one is has sensitive volume of 0.6 cm^3, vented to air, see figure 4.2 (d).

Figure 4.2 Detectors at Lopburi cancer center a) Diode p-type detector, b) Advance Markus (plane parallel) chamber, c) IC 0.3 cm^3 semiflex, d) IC 0.6 cm^3 Farmer chamber.

Table 4.1 Sensitive volume of the employed detectors.

Detectors	Diode type 6008 (PTW-Freiburg)	Markus type 34045 (PTW Freiburg)	IC03 semiflex type 31013 (PTW-Freiburg)	IC Farmer chamber
Sensitive volume	0.0025 mm^3	0.02 cm^3	0.3 cm^3	0.6 cm^3

3. Water phantoms and software for beam scanning

The acquisition system is a PTW MP3 water phantom (PTW Freiburg, Germany) with its own electrometer, position controllers and acquisition software, Mephysto mc^2 version 1.3.1 as shown in Figure 4.3 (a)-(c).

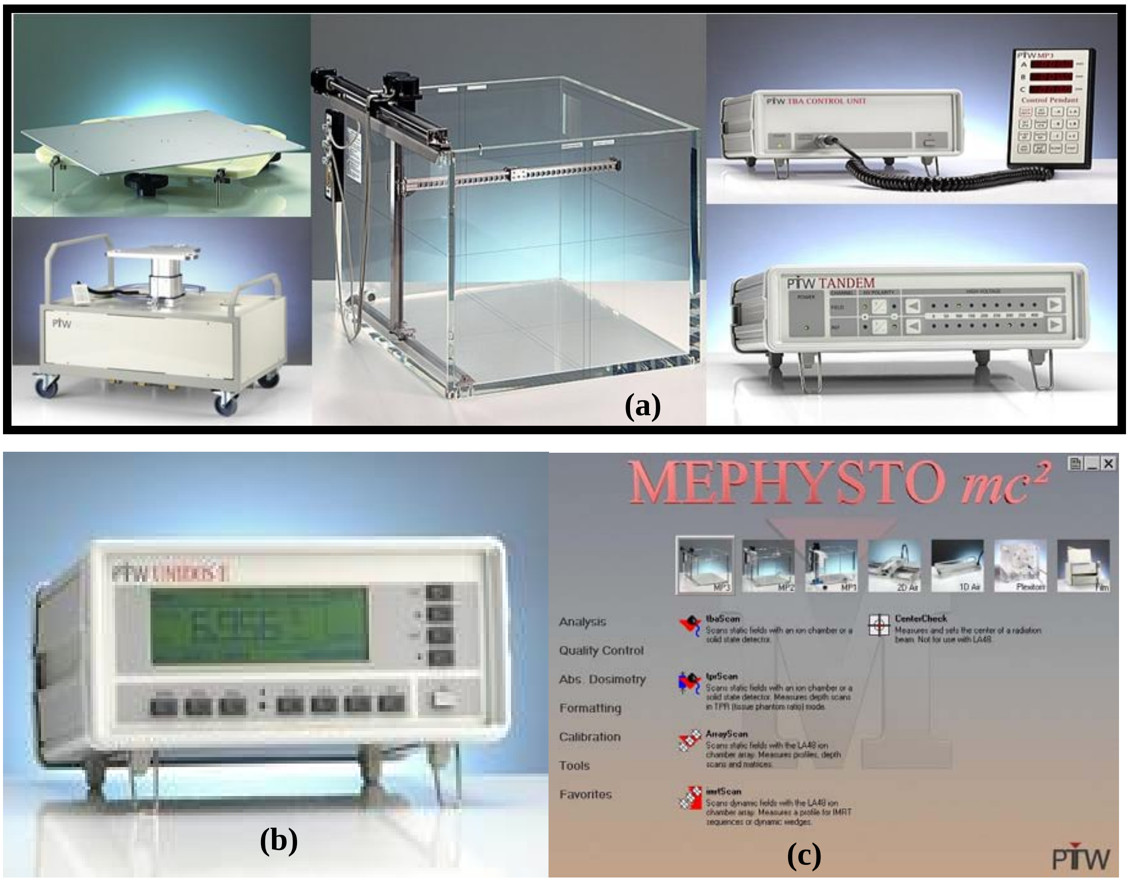

Figure 4.3 PTW-Freiburg scanner at Lopburi cancer center (a) water tank, tandem and control unit, (b) Electrometer PTW UnidosE, (c) MEPHYSTO mc^2 Program.

B. Method

1. Output factor measurement

Output factor for field sizes between 2×2 to 30×30 cm^2 were measured with the diode, IC 0.3 cm^3, IC 0.6 cm^3 and Markus parallel plate detector. The output factors were obtained at 10 cm water depth as the ratio of the detector response for a certain field size and the detector response for the 10×10 cm^2 field with SAD 100 cm. For each irradiation 100 monitor units were used, excluded the plane parallel, that 300 monitor units were used as shown in Figure 4.4. Before measurement, performing quality assurance for machine in radiotherapy was always required such as optical distance index, laser, field size alignment, gantry and collimator angles, etc. The % difference comparison with IC 0.6 cm^3 follow equal (3).

$$\frac{(o/p_x - o/p_{IC})}{o/p_{IC}} \times 100 \qquad (3)$$

where o/p_x is the output factor obtains from any detectors and o/p_{IC} is the output factor obtains from IC 0.6 cm^3.

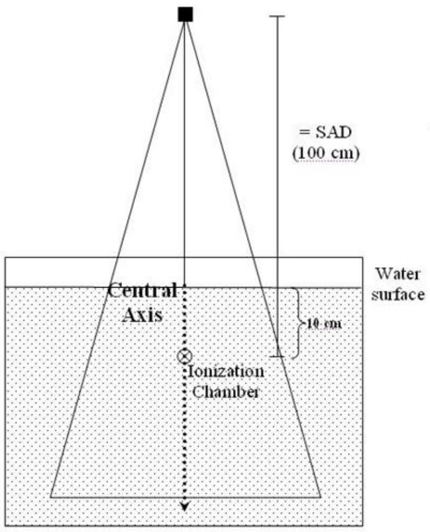

Figure 4.4 Output factors measurement setup

2. Percentage depth dose

The percentage depth dose for field sizes between 2×2 to 30×30 cm^2 were used. The diode, IC 0.3 cm^3 and plane parallel detector were setup by considering the effective point of measurement 0.6 mm from detector tip 9.5 mm and 1.06 mm respectively. Data were acquired using a source-surface distance of 100 cm. Square fields, having sizes of 2 cm, 3 cm, 4 cm, 5 cm, 6 cm, 8 cm, 10 cm, 12 cm, 15 cm, 20 cm, 25 cm, 30 cm were employed for PDD measurement, as shown in Figure 4.5. Depth dose curves, obtained with different dosimeters, were compared for two different parameters: the distance between points with the same dose value in the high gradient region and the percent dose differences in the decreasing part of the curve. Before measurement, performing quality assurance for machine in radiotherapy was always required such as optical distance index, laser, field size alignment, gantry and collimator angle etc. The percent difference is calculated from equation (4).

$$\frac{(DD_x - DD_{diode})}{DD_{diode}} \times 100 \qquad (4)$$

where DD_x is the depth dose measured by any detector and DD_{diode} is the depth dose measured by diode detector.

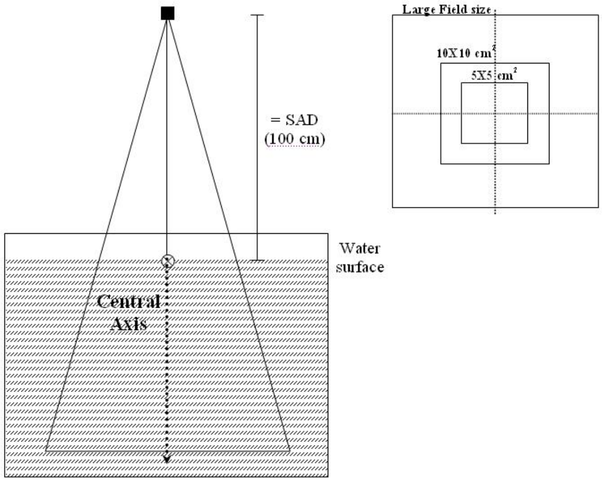

Figure 4.5 Percentage depth dose measurement setup

3. Beam profile measurement

Data were acquired using a source-surface distance of 100 cm. Square fields, having sizes of 2 cm, 3 cm, 4 cm, 5 cm, 6 cm, 8 cm, 10 cm, 12 cm, 15 cm, 20 cm, 25 cm and 30 cm were used. Only the cross plane profile direction was acquired at the depths of maximum dose (1.5 cm), 5 cm and 10 cm, see in figure 4.6. The agreement between the different detectors was evaluated by determining percent relative of the central axis and off-axis, the penumbra 20 – 80% and the penumbra tail. Before measurement, performing quality assurance for machine in radiotherapy was always required such as optical distance index, laser, field size alignment, gantry and collimator angle etc.

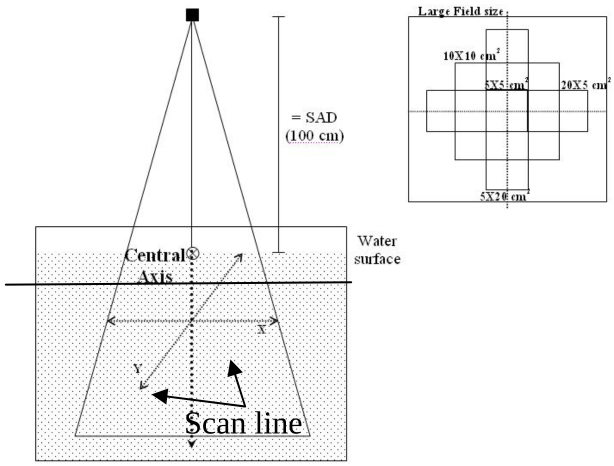

Figure 4.6 Beam profile measurement setup

In this research, the XO mat V film was used to be a reference for the diode detector due to its high spatial resolution especially for penumbra width measurement of the beam profile. After that, diode was used as a reference detector for beam profile and depth dose measurement.

CHAPTER V
RESULTS AND DISCUSSION

Output factors

In this result, IC 0.6 cm^3 was used as a reference detector. The obtained output factors with the percent difference compared with IC 0.6 cm^3, normalized to the 10 × 10 cm^2 field, and are reported in Table 5.1. The output factor using IC 0.3 cm^3 and Markus chamber is in close agreement within 2.2% between 3×3 and 30×30 cm^2 field sizes compared with IC 0.6 cm^3. The diode output factor measurement compared with IC 0.6 cm^3, agrees within 2.1% between 3×3 and 15×15 cm^2 field sizes. The critical discrepancy is found for 2×2 cm^2 field size for any detectors with respect to IC 0.6 cm^3 which is more than 20%. Because a lack of electron equilibrium and high dose gradients are present in the small field, IC 0.6 cm^3 contains too large volume to measure output factor for this kinds of situation which leads to underestimation of the result (Haryanto *et al* 2002). The output factor measured with diode is also concerned especially at large field sizes (> 20×20 cm^2) in which the disagreement is more than 3%. Because diode is the solid state detector which is considered high z material (z of Si =14), the response of this detector considerably increases for the low energy especially larger field sizes due to higher low energy photon fraction (Sauer OA and Willbert 2007).

Table 5.1 Output factor and % difference compared with IC 0.6 cm^3 for 6 MV of Varian 2100 C/D with SAD = 100 cm at 10 cm depth, normalized to 10×10 cm^2 field size.

Field size (cm)	IC 0.6 cm^3	IC 0.3 cm^3		PP		Diode	
		Output factor	% diff compared with IC	Output factor	% diff compared with IC	Output factor	% diff compared with IC
2	0.6245	0.7763	24.3	0.7690	23.1	0.7642	22.4
3	0.8084	0.8263	2.2	0.8247	2.0	0.8050	-0.4
4	0.8605	0.8617	0.1	0.8609	0.1	0.8422	-2.1
5	0.8931	0.8915	-0.2	0.8913	-0.2	0.8750	-2.0
6	0.9204	0.9188	-0.2	0.9180	-0.3	0.9043	-1.7
8	0.9662	0.9642	-0.2	0.9637	-0.3	0.9570	-1.0
10	1.0000	1.0000	0.0	1.0000	0.0	1.0000	0.0
12	1.0315	1.0290	-0.2	1.0292	-0.2	1.0368	0.5
15	1.0662	1.0626	-0.3	1.0636	-0.2	1.0826	1.5
20	1.1076	1.1027	-0.4	1.1067	-0.1	1.1450	3.4
25	1.1392	1.1333	-0.5	1.1402	0.1	1.1959	5.0
30	1.1652	1.1589	-0.5	1.1692	0.3	1.2406	6.5

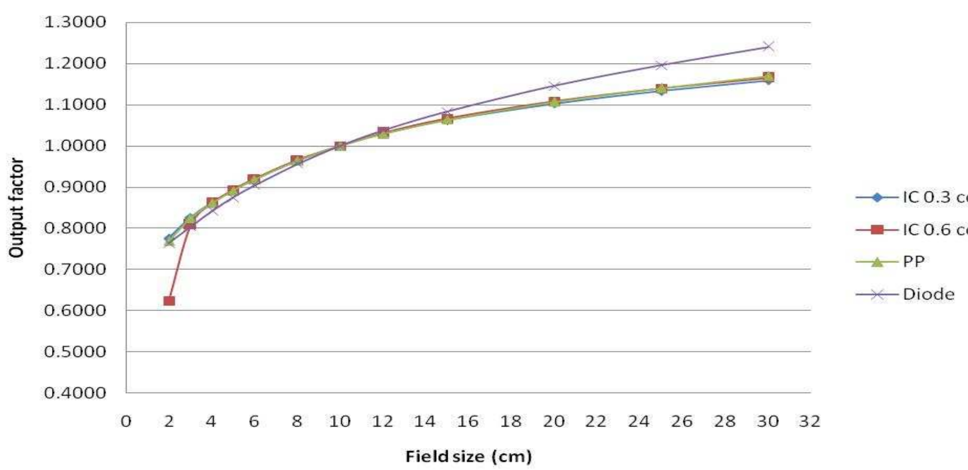

Figure 5.1 Output factor measurements with various field sizes and detectors

Percentage depth dose

Figure 5.2 shows central axis percentage depth dose measured with diodes, IC (0.3 cm^3) and parallel plate chamber for (a) field size of 2×2 cm^2, (b) field size of 10×10 cm^2, and (c) field size of 30×30 cm^2. The signals are normalized to 100% at depth of maximum dose i.e. 1.5 cm depth.

There is some research mentioned that the performance of the diode is equivalent to the diamond detector (Bucciolini M *et al,* 2003). Diamond detector is as good as ideal detector especially for small fields and high dose gradient region because of its high spatial resolution and water-equivalent material (Laub W and Wong T, 2003). Therefore the diode detector is used as a reference in this study.

The largest difference between the detectors with respect to diode detector is seen at the surface (depth = 0 cm) with a relative difference of about 3.5-9.4%, where all the larger detectors (IC 0.3 cm^3 and Markus chamber) overestimate the dose for all field sizes compared with diode measurement due to their volume effect (Bucciolini *et al* 2003) as shown in Table 5.2 and Fig 5.2. However they show the best agreement with the diode within 2 % of relative difference at depth of 10 cm for field sizes of 2×2 and 10×10 cm^2. Nevertheless diode overestimates the dose at larger depth i.e. 10 and 30 cm which is more than 2% of relative difference for field size of 30×30 cm^2 because the quantity of low energy are higher at larger depth and field size leads to over-response of diode measurement.

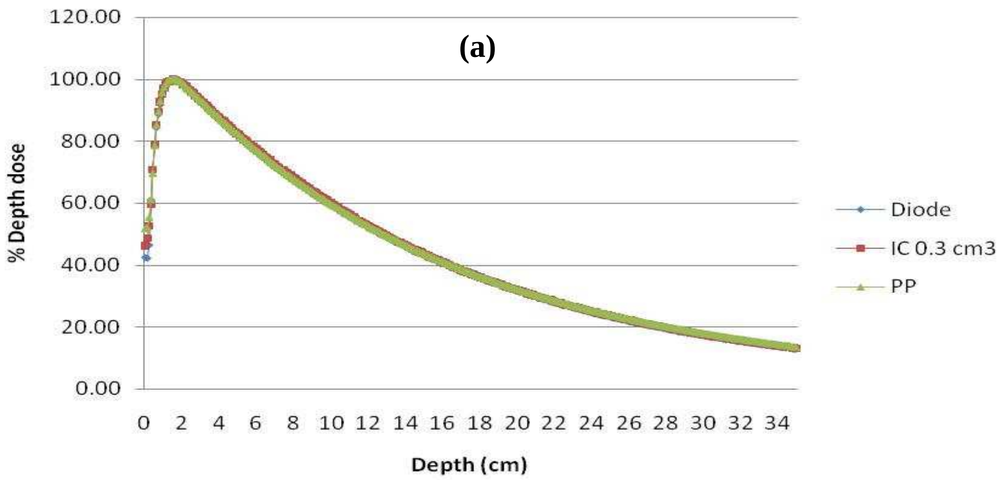

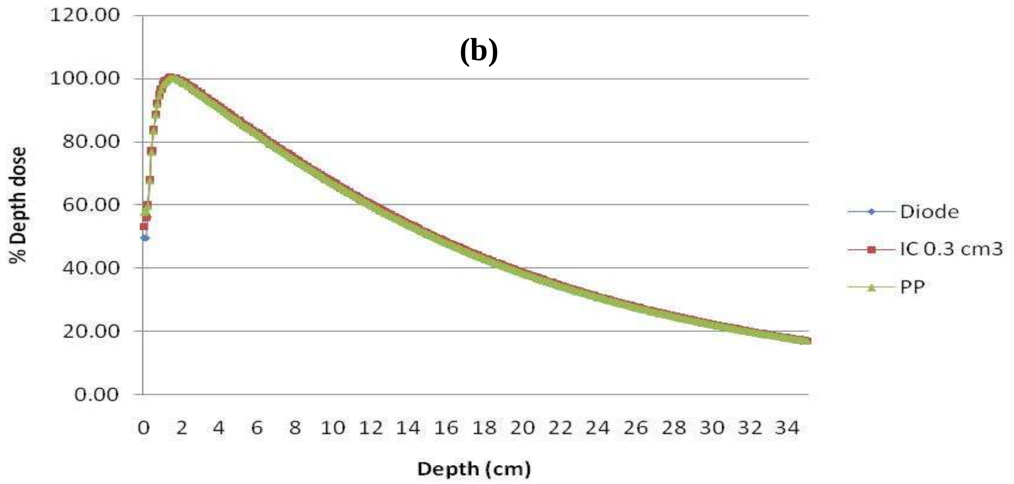

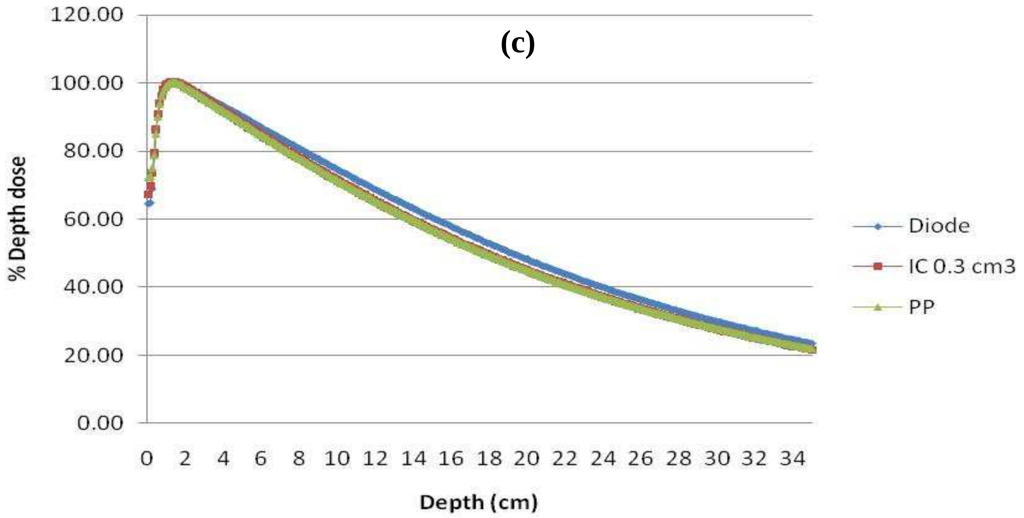

Figure 5.2 Percentage depth dose for (a) 2×2 cm^2 field size, (b) 10×10 cm^2 field size, and (c) 30×30 cm^2 field size.

Table 5.2 The relative difference of the percentage depth dose at depth 0, 10, and 30 cm for field size 2×2, 10×10, and 30×30 cm^2 with respect to diode measurement

Depth (cm)	2×2 cm^2		10×10 cm^2		30×30 cm^2	
	IC 0.3 cm^3	PP	IC 0.3 cm^3	PP	IC 0.3 cm^3	PP
0	3.7	9.4	3.5	8.0	2.4	7.6
10	-0.5	-0.5	-0.5	-0.8	-3.3	-3.5
30	0.6	-0.2	0	-0.2	-2.4	-2.1

Beam profile

The XO mat V film was used for a reference detector for diode measurement for filed size of 2×2, 10×10, and 15×15 cm^2 at depth of 1.5 cm and field size of 10×10, 20×20, and 30×30 cm^2 at depth of 10 cm as shown in Table 5.3.

Table 5.3 The penumbra width and the penumbra tail between film and diode comparison for field size of 2×2, 10×10, and 15×15 cm^2 at depth of 1.5 cm and field size of 10×10, 20×20, and 30×30 cm^2 at depth of 10 cm.

Depth (cm)	Field size (cm)	Penumbra width (cm)		Penumbra tail (%relative dose)	
		XV film	Diode	XV film	Diode
1.5	2×2	0.24	0.24	0.73	0.8
	5×5	0.25	0.25	1.3	2.1
	10×10	0.34	0.26	3.5	3.7
	15×15	0.36	0.26	4.4	5.1
10	10×10	0.43	0.4	6.8	7.9
	20×20	0.71	0.61	10.0	12.0
	30×30	0.80	0.89	10.7	14.5

The spatial resolution of XV film depends on the scanner resolution. In this case, the 300 dot per inch (0.08 mm/pixel) of the Vidar 12$^+$ scanner was used for scanning and Image J program was employed to analyze the data. The penumbra widths between XV film and diode are excellent agreement within 1 mm. Also the penumbra tail between these two detectors is well matched except depth at 10 cm with large field sizes (20×20 and 30×30 cm^2).

Figure 5.3-5.7 show the beam profiles obtained with the different detectors for the 2×2, 5×5, 10×10, 20×20, and 30×30 cm^2 field size respectively of the depth of (a) 1.5 cm, (b) 5 cm, and (c) 10 cm in a 6 MV photon beam at 100 cm SSD. The profiles have been normalized to 100% at the central axis for each depth and field size.

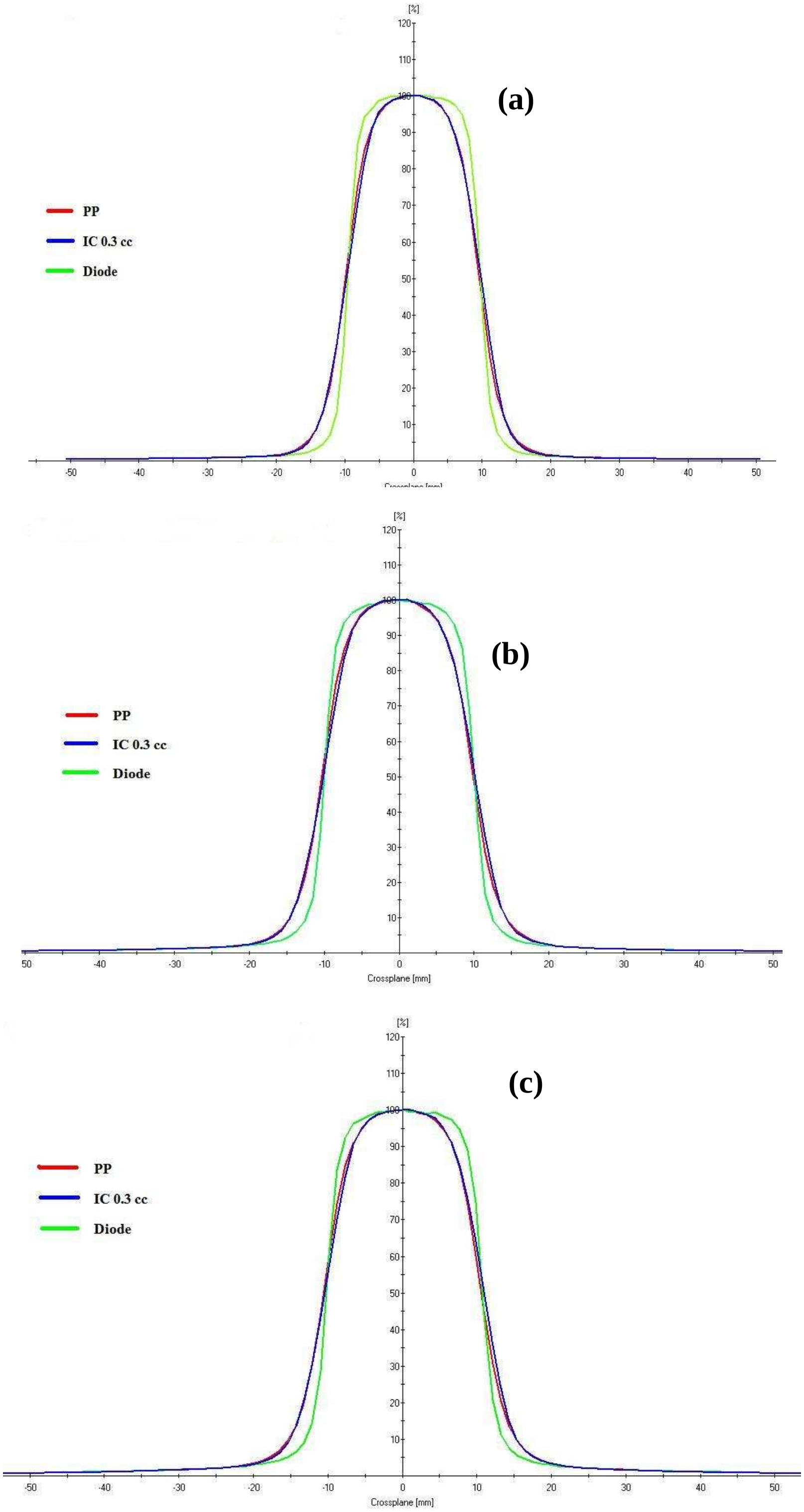

Figure 5.3 Beam profiles for the 2×2 cm^2 field size at (a) depth 1.5 cm, (b) depth 5 cm, and (c) depth 10 cm, 100 cm SSD in a 6 MV photon beam measured with parallel plate, IC 0.3 cc, and diode detectors in water.

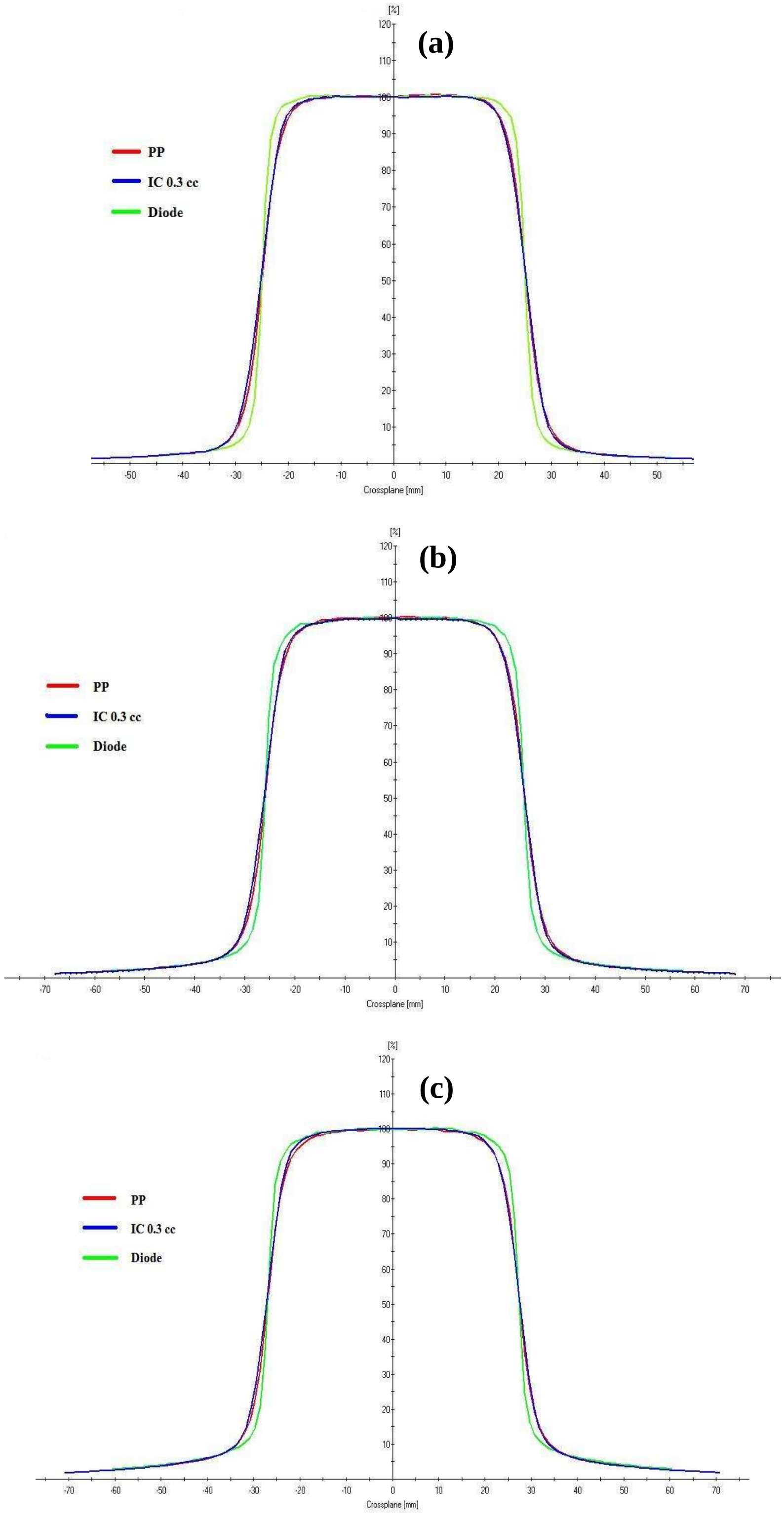

Figure 5.4 Beam profiles for the 5×5 cm^2 field size at (a) depth 1.5 cm, (b) depth 5 cm, and (c) depth 10 cm, 100 cm SSD in a 6 MV photon beam measured with parallel plate, IC 0.3 cc, and diode detectors in water.

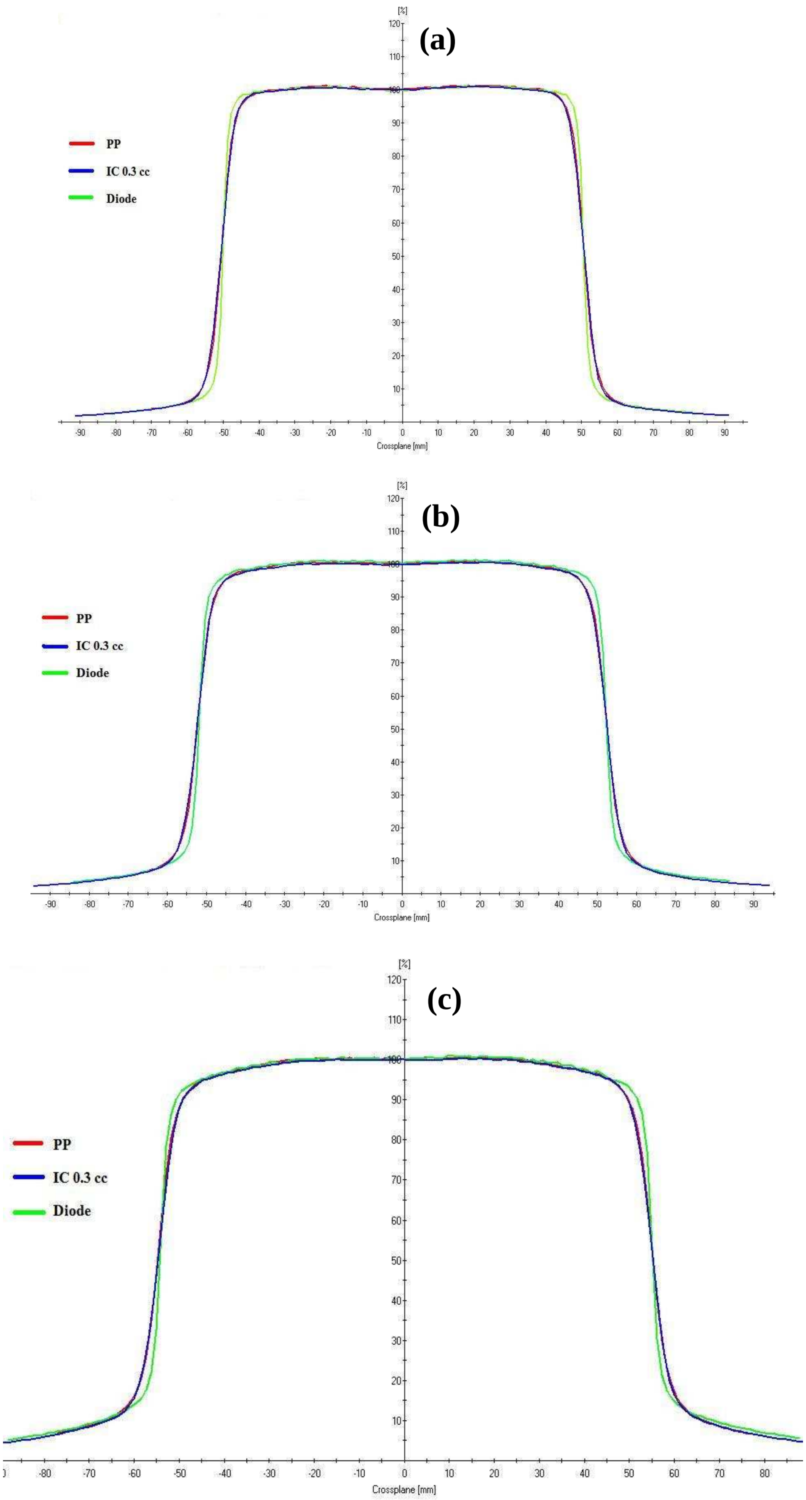

Figure 5.5 Beam profiles for the 10×10 cm^2 field size at (a) depth 1.5 cm, (b) depth 5 cm, and (c) depth 10 cm, 100 cm SSD in a 6 MV photon beam measured with parallel plate, IC 0.3 cc, and diode detectors in water.

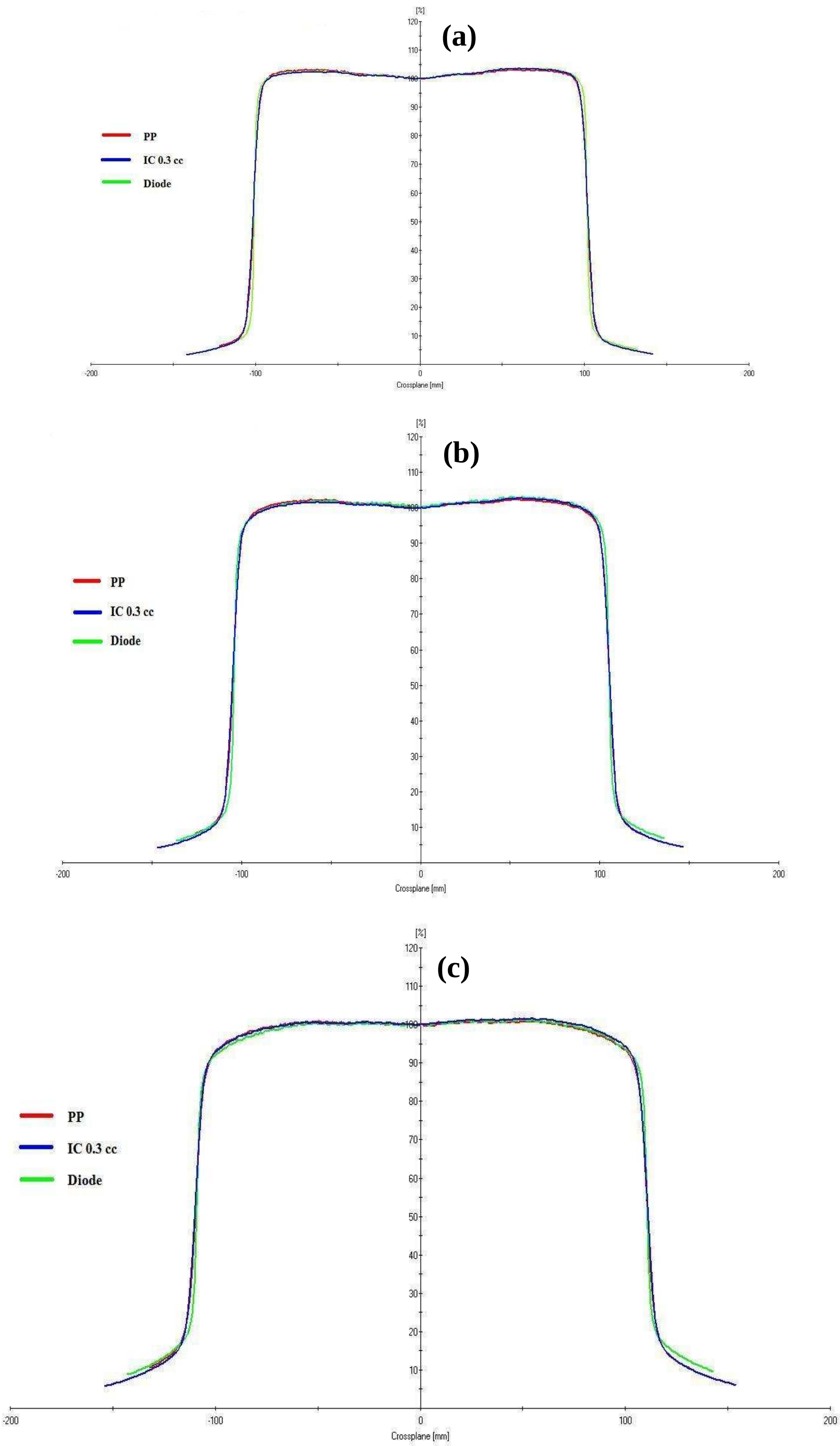

Figure 5.6 Beam profiles for the 20×20 cm^2 field size at (a) depth 1.5 cm, (b) depth 5 cm, and (c) depth 10 cm, 100 cm SSD in a 6 MV photon beam measured with parallel plate, IC 0.3 cc, and diode detectors in water.

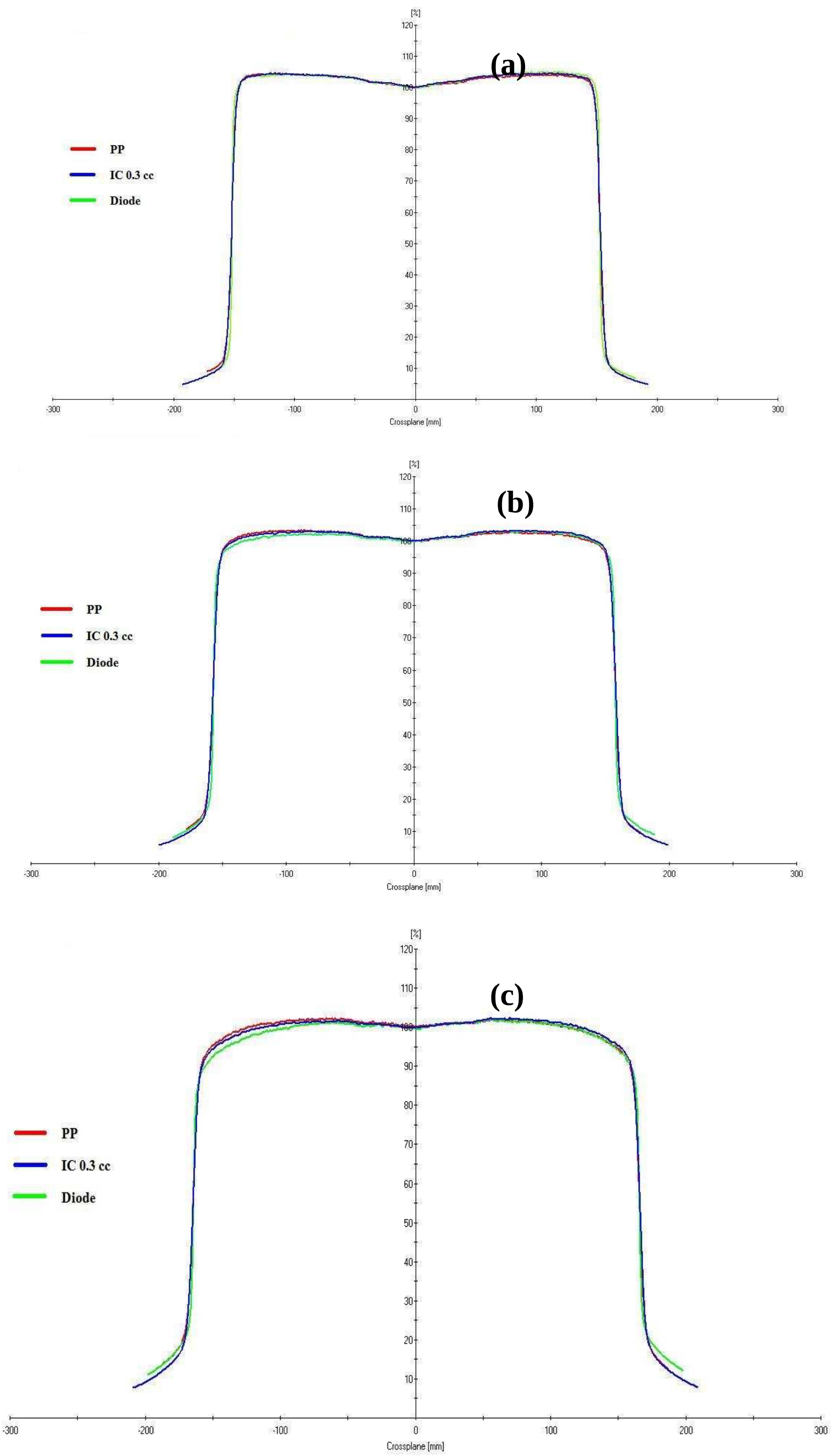

Figure 5.7 Beam profiles for the 30×30 cm^2 field size at (a) depth 1.5 cm, (b) depth 5 cm, and (c) depth 10 cm, 100 cm SSD in a 6 MV photon beam measured with parallel plate, IC 0.3 cm^3, and diode detectors in water.

As expected, diode obtains the higher spatial resolution due to its smaller sensitive volume, its penumbra width is narrower than the Markus parallel plate chamber and IC 0.3 cm^3 for all field sizes at any depths as shown in Figure 5.8. However diode suffers from the sensitivity to the low energy due to high z material (z of Si = 14), the trend of the diode penumbra width increases especially at larger field size and depth as shown in Figure 5.8 (c). Results concerning the %relative dose of the penumbra tail which contains some amount of low energy are reported in Figure 5.9. As expected for the diode measurement, it shows higher response at larger depth (5 and 10 cm) and larger field size (from 15×15 cm^2).

Both of IC 0.3 cm^3 and Markus parallel plate chamber suffer from an insufficient spatial resolution compared with diode measurement for all filed sizes and depths. Their maximum difference of the penumbra width compared with penumbra width measured with diode is about 3 mm. Moreover comparison between IC 0.3 cm^3 and Markus parallel plate chamber was found that IC 0.3 cm^3 gives slightly larger penumbra width due to bigger sensitive volume as expected. Nevertheless Markus parallel plate chamber is the air equivalent but it has larger surface area which is non-tissue equivalent material facing the beam as a result of more sensitive to the low energy which leads to higher value of the penumbra tail compared with IC 0.3 cm^3.

(a)

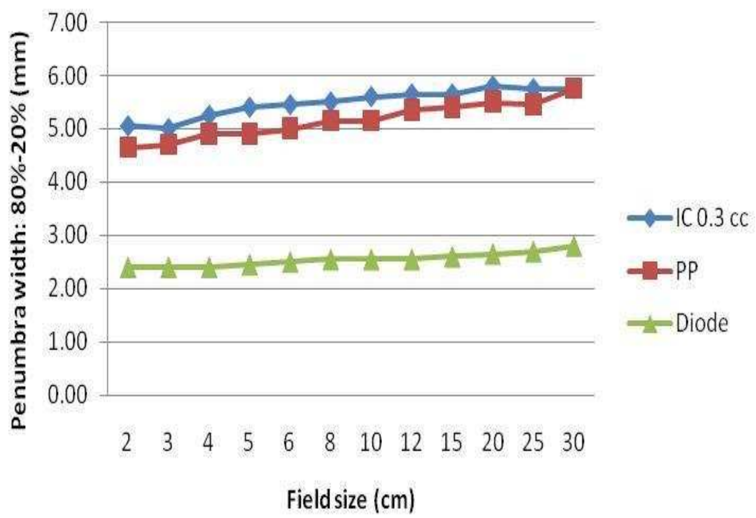

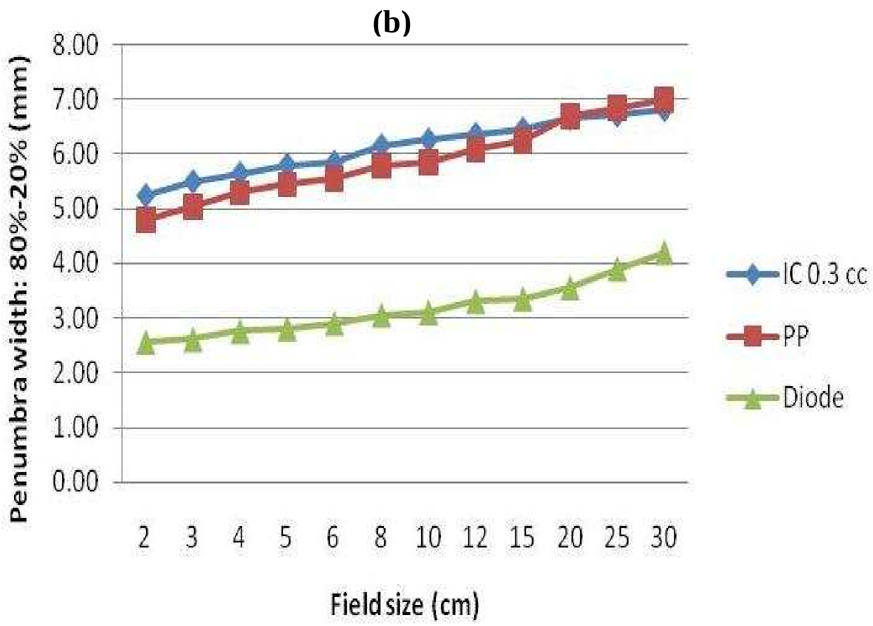

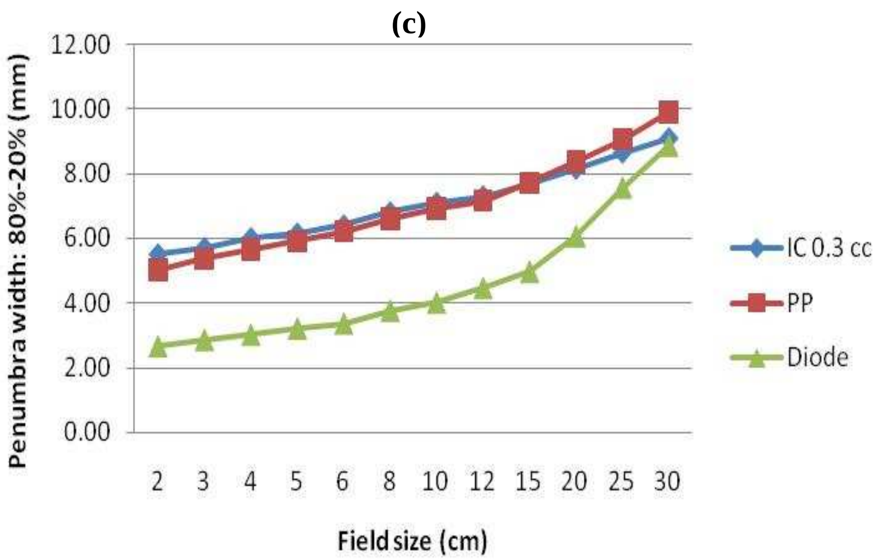

Figure 5.8 Penumbra widths (80%–20%) measured with IC 0.3 cm^3, Parallel plate (PP), and Diode detectors at depth of (a) 1.5 cm, (b) 5 cm, and (c) 10 cm for 2, 3, 4, 5, 6, 8, 10, 12, 15, 20, 25, 30 cm^2 field sizes at 100 cm SSD in water for a 6 MV photon beam.

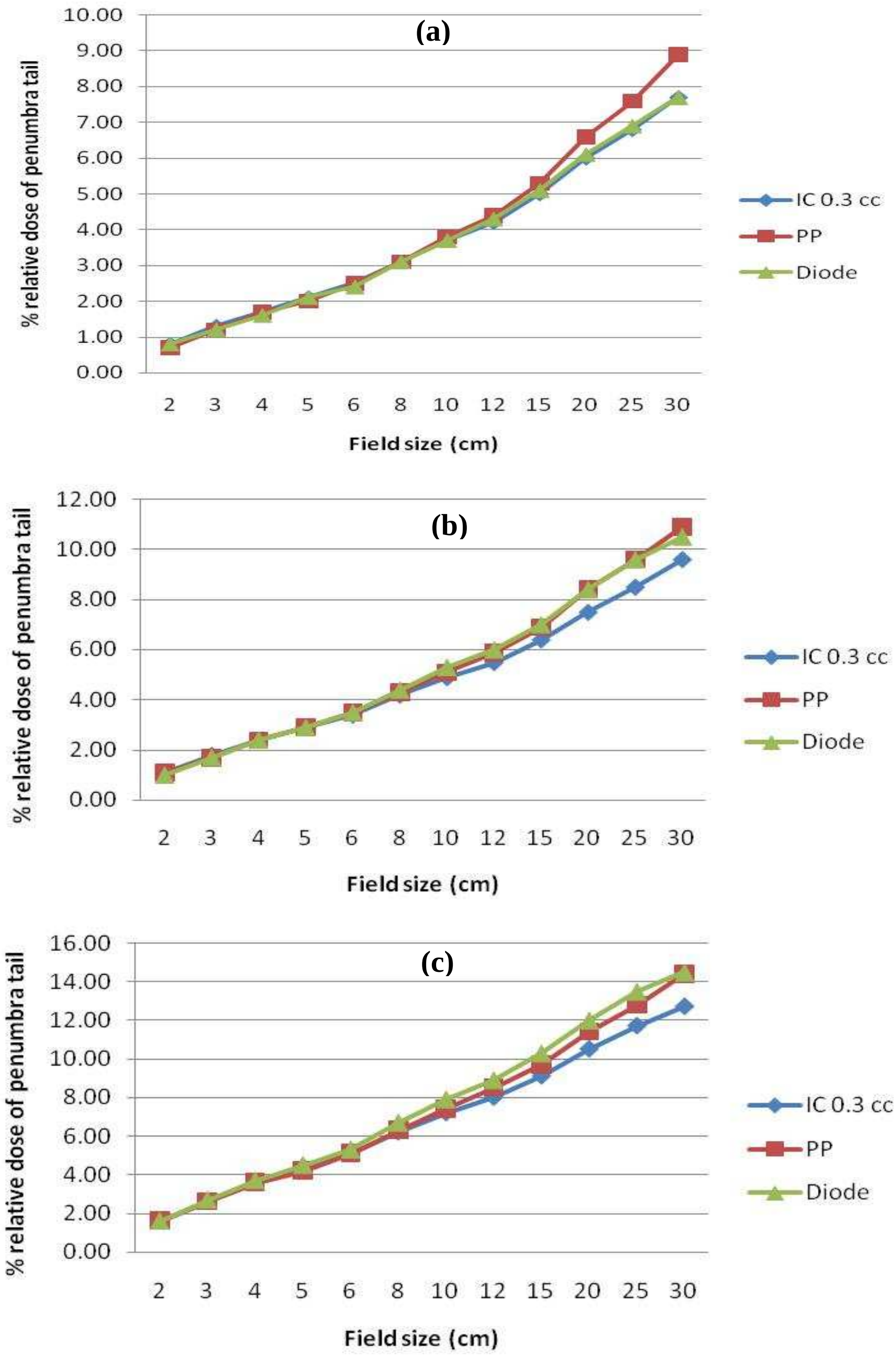

Figure 5.9 Penumbra tail (%relative dose from the border of the field size 2 cm) measured with IC 0.3 cm^3, Parallel plate (PP), and diode detectors at depth of (a) 1.5 cm, (b) 5 cm, and (c) 10 cm for 2, 3, 4, 5, 6, 8, 10, 12, 15, 20, 25, and 30 cm^2 field sizes at 100 cm SSD in water for a 6 MV photon beam.

CHAPTER VI
SUMMARY AND CONCLUSIONS

A comparison of the response of different dosimeters in a 6 MV photon beam has been performed. The detectors used were IC 0.6 cm^3, IC 0.3 cm^3, Markus parallel plate chamber, and diode. For output factor measurement, IC 0.3 cm^3, Markus parallel plate chamber, and diode were used with respect to IC 0.6 cm^3. However for beam profile and depth dose measurement, IC 0.3 cm^3, Markus parallel plate chamber were used with respect to the diode measurement due to its high spatial resolution comparable with XV film measurement.

The IC 0.3 cm^3 and Markus chamber measures output factors close to those with IC 0.6 cm^3 except 2×2 cm^2 field size. The output factor measured by IC 0.6 cm^3 obtained lowest value because IC 0.6 cm^3 itself has the biggest sensitive volume, it could not cope with the situations of electronic disequilibrium and high dose gradient situation for small field (2×2 cm^2). The diode detector is comparable with IC 0.6 cm^3 for output factor measurement for field size between 3×3 and 12×12 cm^2. The field size larger than 12×12 cm^2 is considerable overestimation due to the high content of low-energy photons.

The depth dose for all field sizes agree well for the IC 0.3 cm^3 and Markus parallel plate chamber compared with diode except surface dose and distal region. The surface dose measurement by IC 0.3 cm^3 and Markus parallel chamber is higher than the value of diode, again due to their larger sensitive volume. The maximum of the %relative difference of the surface dose measurement compared with diode is 3.7% and 9.4% for field size 2×2 cm^2 measured by IC 0.3 cm^3 and Markus parallel plate chamber respectively. However diode is not tissue equivalence as a result it measures a slightly higher dose measurements at the distal region of the depth dose curve with the maximum difference about 3.3% for 30×30 cm^2 at depth 10 cm compared with IC 0.3 cm^3.

The IC 0.3 cm^3 and Markus chamber detect a penumbra width that is broader than diode measurement due to their finite size, while diode obtains smaller penumbra width due to smaller sensitive volume. However diode and Markus parallel plate chamber slightly overestimate the %relative dose of the penumbra tail compared with IC 0.3 cm^3 at the maximum difference about 2%.

In conclusion, the IC 0.3 cm^3 and Markus parallel plate chamber agreed with IC 0.6 cm^3 for output factor measurement except smaller field size than 3×3 cm^2. Their surface dose and penumbra measurement compared with diode obtained higher value due to their finite size of the sensitive volume. However diode is slightly over-response at the distal region of the depth dose curve measurement due to its non tissue equivalence. It is difficult to decide which detector gives the proper beam data measurement. Nevertheless these detectors are suitable for the 3D conformal radiotherapy technique. It is required further study to obtain the suitable detector to measure dose in the small fields and high dose gradient region.

Table 6.1 summary result of Output factor for other detector

Field size (cm^2)	Detector	Cause	Due to
2×2	IC 0.6 cm^3	Underestimation of Output factor.	Lateral electronic disequilibrium due to averaging effect.
3×3 to 30×30	IC 0.3 cm^3 and PP	Agree within 2.2%	
3×3 to 15×15	Diode	Agree within 2.1%	
Above 20×20	Diode	Overestimation of Output factor.	Diode has high z material and large field size has high low energy photon.

Table 6.2 the summary result of Profile for other detector

Field size (cm^2)	Depth	Detector	Cause	Due to
All FS	Any depth	Diode	Penumbra width is narrower than IC 0.3 cm^3 and PP.	Diode has high z material and small sensitive volume.
All FS	All depth	IC 0.3 cm^3 and PP	They suffer from an insufficient spatial resolution compared with diode	They are large sensitive volume
All FS	All depth	PP	Penumbra width is narrower than IC 0.3 cm^3	PP is the air equivalent but it has large surface area which is non tissue equivalent material
Large FS	10 cm	Diode	Penumbra width and %relative dose of penumbra tail increase	High low energy of large field size and high z material of diode

Table 6.3 the summary result of percentage depth dose for other detector

Field size (cm^2)	Depth	Detector	Cause	Due to
All FS	surface	IC 0.3 cm^3 and PP	Overestimation of the dose compared with diode	Volume effect
2×2 to 10×10	10 cm	IC 0.3 cm^3 and PP	Agree within 2%	
30×30	10 -30 cm	Diode	Overestimation of the dose	Diode has high z and field size and depth increase so high low energy due to energy absorption coefficient ratio

REFERANCES

1. Evans MDC. Computerized treatment planning systems for external photon beam radiotherapy. In: Podgorsak EB. Radiation oncology physics: a handbook for teachers and students. Vienna: IAEA; 2005. 387 – 405.
2. Khan FM. Treatment planning: isodose distributions . In: Khan FM . The physics of radiation therapy. Williams & Wilkins; 1994. 240-246.
3. Podgorsak EB. External photon beam : Physical aspects. In: Podgorsak EB. Radiation oncology physics: a handbook for teachers and students. Vienna: IAEA; 2005. 161 – 216.
4. Izewska J, Rajan G. Radiation Dosimeters. In: Podgorsak EB. Radiation oncology physics: a handbook for teachers and students. Vienna: IAEA; 2005. 71 – 99.
5. Vicente FG, Bejar M, Perez L, Torres J. Clinical impact of the detector size effect in 3D-CRT. Radiotherapy and Oncology 2005; 74: 315-22.
6. Haryanto F,Fippel M, Laub W, Dohm O, Nusslin F. Investigation of Photon beam output factors for conformal radiation therapy-Monte Carlo simulations and measurements. Phys Med Biol 2002; 47 : N133-N143.
7. Bucciolini M, Buonamici FB, Mazzocchi S, Angelis CD, Oniri S, Cirrone GAP. Diamond detector versus silicon diode and ion chamber in photon beams of different energy and field size. Med Phys 2003; 30: 2149-54.
8. Laub WU, Wong T. The volume effect of detector in the dosimetry of small fields used in IMRT. Med Phys 2003; 30(3): 341-7.
9. Rustgi SN. Evaluation of the dosimetric characteristics of a diamond detector for photon beam measurements. Med Phys 1995; 22(5): 567-70.

APPENDIX

Table 7.1 to 7.6 Penumbra width (80-20%) in mm and penumbra tail (%relative dose from the border of the field size 2 cm) for a 6 MV photon beam as measured by the IC 0.3 cc, parallel plate chamber (PP), and diode. XO mat V film was used as a standard detector compared with diode measurement of 2×2, 5×5, and 10×10 cm field size at depth of 1.5 cm and of 10×10, 20×20, and 30×30 cm field size at depth of 10 cm. (move to appendix)

Table 7.1 Penumbra width (80%-20%) at depth 1.5 cm

FS	depth 1.5 cm			
	IC 0.3 cc	PP	Diode	XV film
2	5.05	4.65	2.40	2.40
3	5.00	4.70	2.40	
4	5.25	4.90	2.40	
5	5.40	4.90	2.45	2.50
6	5.45	5.00	2.50	
8	5.50	5.15	2.55	
10	5.60	5.15	2.55	3.40
12	5.65	5.35	2.55	
15	5.65	5.40	2.60	3.60
20	5.80	5.50	2.65	
25	5.75	5.45	2.70	
30	5.75	5.75	2.80	

Table 7.2 Penumbra width (80%-20%) at depth 5 cm

FS	depth 5 cm		
	IC 0.3 cc	PP	Diode
2	5.25	4.80	2.55
3	5.50	5.05	2.60
4	5.65	5.30	2.75
5	5.80	5.45	2.80
6	5.85	5.55	2.90
8	6.15	5.80	3.05
10	6.25	5.85	3.10
12	6.35	6.10	3.30
15	6.45	6.25	3.35
20	6.65	6.70	3.55
25	6.70	6.85	3.90
30	6.80	7.00	4.20

Table 7.3 Penumbra width (80%-20%) at depth 10 cm

S	depth 10 cm			
	IC 0.3 cc	PP	Diode	XV film
2	5.50	5.00	2.65	
3	5.70	5.35	2.85	
4	6.00	5.65	3.00	
5	6.15	5.90	3.20	
6	6.40	6.20	3.35	
8	6.80	6.60	3.75	
10	7.10	6.90	4.00	4.30
12	7.30	7.15	4.45	
15	7.70	7.70	4.95	
20	8.15	8.35	6.05	7.10
25	8.65	9.05	7.55	
30	9.10	9.90	8.85	8.00

Table 7.4 Penumbra tail at depth 1.5 cm

FS	penumbra tail 1.5 cm			
	IC 0.3 cc	PP	Diode	XV film
2	0.80	0.70	0.80	0.73
3	1.30	1.20	1.20	
4	1.70	1.70	1.60	
5	2.10	2.00	2.10	1.26
6	2.50	2.50	2.40	
8	3.10	3.10	3.10	
10	3.70	3.80	3.70	3.50
12	4.20	4.40	4.30	
15	5.00	5.30	5.10	4.40
20	6.00	6.60	6.10	
25	6.80	7.60	6.90	
30	7.70	8.90	7.70	

Table 7.5 Penumbra tail at depth 5 cm

FS	penumbra tail 5 cm		
	IC 0.3 cc	PP	Diode
2	1.10	1.10	1.00
3	1.80	1.70	1.70
4	2.40	2.40	2.40
5	2.90	2.90	2.90
6	3.40	3.50	3.50
8	4.20	4.30	4.40
10	4.90	5.10	5.30
12	5.50	5.90	6.00
15	6.40	6.90	7.00
20	7.50	8.40	8.40
25	8.50	9.60	9.60
30	9.60	10.90	10.50

Table 7.6 Penumbra tail at depth 10 cm

FS	penumbra tail 10 cm			
	IC 0.3 cc	PP	Diode	XV film
2	1.60	1.60	1.60	
3	2.60	2.60	2.70	
4	3.60	3.60	3.70	
5	4.40	4.20	4.50	
6	5.10	5.10	5.30	
8	6.20	6.30	6.70	
10	7.20	7.40	7.90	6.80
12	8.00	8.50	8.90	
15	9.10	9.70	10.30	
20	10.50	11.40	12.00	10.00
25	11.70	12.80	13.50	
30	12.70	14.40	14.50	10.70

BIOGRAPHY

NAME	Mr. Thepphithak Watthanasarn
DATE OF BIRTH	24 October 1974
PLACE OF BIRTH	Kalasin, Thailand
INSTITUTIONS ATTENDED	Medical and Public Health Technology College, 1996: Technical level of Radiographic Technology
	Thepsatri Rajabhat University, 1999: Bachelor of Science (Health Science)
	Mahidol University, 2003: Bachelor of Science (Radiological Technology)
	Mahidol University, 2008: Master of Science (Medical Physics)
POSITION&OFFICE	11/1 Lopburi Cancer Center, Lopburi, Thailand
	Position: Medical Physicist
	Tel. Office 036-621800 ext 131,314
	Mobile Phone: 089-0657890
	E-mail: Thepphithak@gmail.com
HOME ADDRESS	109/6 Lopburi Lopburi, Thailand